

UNIVERSITY OF NAIROBI
DEPARTMENT OF PHYSICS



**MONITORING EVOLUTION OF COASTLINE ALONG MTO
TAMAMBA DELTA IN KENYA NORTH COAST USING
SATELLITE IMAGES.**

By

AKETCH, NEWTON DANIEL (BED) SC. HON
I56/68369/2013

A thesis submitted in partial fulfillment of requirements of the award of the degree
of Master of Science (Physics) of the University of Nairobi.

June, 2023

DECLARATION

I hereby declare that this thesis is my original work and has not been submitted to any university for examination or award of a degree. All sources of information and references used in this work have been acknowledged and cited in accordance with the University of Nairobi's requirements.

Signature



Date 29/06/2023

Daniel Newton Aketch

The undersigned supervisors certify that they have read and hereby recommend for acceptance by the University of Nairobi the thesis in fulfillment of the requirements for the degree of Master of Science (Physics):

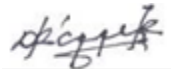
Professor Collins Mito

Department of Physics, University of Nairobi

P. O. Box 30197-00100 Nairobi Kenya

collins@uonbi.ac.ke

Signature



Date 29/06/2023

Professor Giovanni Laneve

Università di Roma 'La Sapienza' Via Salaria, 851- 00138, Roma

giovanni.laneve@uniroma1.it

Signature



Date 02/07/2023

Dedication

I dedicate this thesis to my Dad and Mum; they have helped me learn how to be independent and instilled in me a spirit of perseverance and self-drive. This thesis is also dedicated to my wife and children, who have been by my side during the entire journey of my master's degree.

Abstract

Coastal zones are the epicenter of economic activities in most developing countries in the world hence are bound to change. With advancement in technology monitoring such degradation has become critical subject for scientific research. This study reports a remarkable shoreline change; an aftermath of hydrodynamic effects and human influence on the Kenyan coastline. The sequential accumulation of sediments on Kenya North coast over the past three decades (1990-2021) using Remote sensing and GIS is tracked. Literature on this chronological evolution and its impacts along this coastline is meagre; it is therefore anticipated that the outcome of this study will initiate an elaborate probe into circumstances that contributed to landscape change along this coast. Multispectral Landsat and Sentinel-2 images respectively, display a prograding beach along Mto Tamamba Delta (Kenyan North Coast) a consequence of coastal erosion. These change in coastal morphology poses a threat to marine ecosystems, riparian communities and tourism industry. Prior reports indicate that research work done along this coastline were by field survey. This study is aimed at monitoring coastal erosion and accretion using satellite sensors. To achieve these, coastline data for these years were drawn numerically with the aid of RS and Arc GIS on ENVI 5.3 software. Maximum likelihood and Spectral angular mapper algorithms were used to classify the images due to their threshold input ability that ensures optimum classification results. Time series methodology on classified endmembers was then used to infer the presence of erosion and accretion. Using the image subset technique, areas prone to erosion and accretion within the coastal datum were identified and cut. The patterns of spatiotemporal trend of these endmembers were effectively employed to corroborate these findings. To explain reasons for change, time series analysis and confusion matrix were used. Change in distribution of endmembers over the 31 years' period was assessed using thematic change technique; an approach not previously applied in this study area. From the classified Mto Tamamba image, the pixel coverage area for each endmember was extracted. The regression analysis from class statistics obtained from Mto Tamamba area for bare land and water showed a correlation with $R^2=0.5138$ with a P-value < 0.005 on Landsat data. On the other hand, Sentinel-2 classified image a correlation of $R^2= 0.7857$ for the same endmembers. Validation using field campaign data gave an overall accuracy of 84% and kappa coefficient of 0.799 for Landsat while for sentinel-2 an overall accuracy of 88% and Kappa coefficient of 0.849. The fact that validation of resampled classified Landsat image using a higher spatial resolution satellite (Sentinel-2) gave a better result of 92% implies that adoption of higher resolution data as validation process can aid in assessing impact of resolution on classification results.

Keywords: Remote sensing, Landsat, Coastal evolution, Accretion, Erosion, GIS, Monitoring.

Acknowledgement

I want to start by thanking my supervisors, Professors Collins O. Mito (University of Nairobi) and Giovanni Laneve of the University of Rome, for their supervision, support, constructive criticism, and direction during my research.

Secondly, I want to express my gratitude to the University of Nairobi for the scholarship award. I would also want to thank the entire fraternity of Physics Department for their friendship and moral support. Additionally, I thank Jephther Ondieki and Japheth Aseko, both PhD remote sensing students; for their encouragement and technical support.

Of course, without the generous help, support, and prayers of my cherished wife, my father, and my mother, this effort would not have been a success. I owe them a lot. They encouraged me when I felt like giving up. My wife deserves special recognition for taking care of my kids in my absence during the entire study period.

Finally, I praise the All-Powerful God for His love. He granted me good health, the strength to continue, and everything I required to conduct my study. I shall always praise his holy name!

Table of Contents

DECLARATION	i
Dedication	ii
Abstract	iii
Acknowledgement	iv
Table of Contents	v
List of Figures	viii
List of Tables	viii
List of Abbreviations	ix
CHAPTER 1. INTRODUCTION	1
1.1 Background	1
1.2 Statement of research Problem.	4
1.3 General Objective	5
1.3.1 Specific objective	5
1.3.2 Hypothesis.....	6
1.4 Justification and Significance	6
1.5 Area of study.....	7
CHAPTER 2. LITERATURE REVIEW	10
2.1 Remote sensing technology and application techniques	10
2.1.1 Developments in Remote Sensing Technologies	10
2.1.2 Shoreline Extraction and Change Detection	11
2.1.3 Shoreline Mapping Techniques	13
2.2 Coastal Environmental issues.	14
2.2.1 Coastal erosion and accretion.	14
2.2.2 Sea level rise.	18
2.2.3 Desalination Process.	19
CHAPTER 3. THEORETICAL BACKGROUND.....	20
3.1 Change detection techniques.....	20

3.1.1 Image differencing	20
3.1.2 Clouds and cloud shade removal	21
3.2 Object Detection and Discrimination.....	22
3.3 Vegetation Indices	23
3.3.1 Normalized Difference Vegetation Index (NDVI)	24
3.4 Types of classification	25
3.4.1 Supervised Classification.....	25
3.4.2 Unsupervised classification.....	28
3.5 Image enhancement	28
3.5.1 Image segmentation techniques	28
3.5.2 Conversion of image to RGB	29
CHAPTER 4. MATERIALS AND METHODOLOGY.....	30
4.1 Acquisition of Images.	30
4.2 Image pre-processing	32
4.2.1 Atmospheric correction.....	32
4.2.2 Layer stacking	32
4.2.3 Reprojection	33
4.2.4 Cloud removal.....	33
4.3 Image processing	33
4.3.1 Extraction of signatures (endmember file).....	34
4.3.2 Data training.....	34
4.3.4 Image classification.....	35
Flow chart	36
4.4 The concept of Accuracy assessment.....	37
CHAPTER 5. RESULTS AND DISCUSSION	38
5.1 Classified Landsat Data	38
5.2 Thematic change between 1990 and 2021	40
5.3 Change detection statistics for Landsat between 1990 and 2021	42
5.4 Linear regression plots showing area in square Km covered by each endmember for Landsat data.	44
5.5 Correlation plots for Land cover types.	46

5.6 Classified Sentinel-2 Data.....	48
5.7 Thematic change detection for Sentinel 2 data	50
5.8 Change detection statistics for Sentinel-2 between 2015-2021	51
5.9 Linear regression plots showing area in square Km covered by each endmember for Sentinel data	54
5.10 Accuracy assessment report for classified images	57
5.10.1 Satellite overpass	60
5.10.2 Validation results	60
5.11 Resampling of Landsat to 10m resolution	62
5.11.1 Resampling procedure.....	62
5.11.2 Confusion matrix after resampling	63
5.12 Discussion.....	64
5.13 Limitations	66
CHAPTER 6. CONCLUSION AND RECOMMENDATIONS.	67
6.1 Conclusion	67
6.2 Recommendations.....	68
References	69

List of Figures

Figure 1: Mangrove Forest at the beach of Bwana Saidi in Marereni Location (Magarini sub-county) source-photo by Japheth Aseko	3
Figure 2: Map showing RGB image of study area (Mto Tamamba) encircled (Adapted from (Latawiec and Agol, 2015) , KMFRI).	9
Figure 3: Reflected Solar radiation being detected by satellite. (source – https://www.crisp.nus.edu.sg). .	11
Figure 4: A section of piled eroded sediments from the ocean along the shores of Bwana Saidi beach in Magarini Sub-County (Kilifi County).-Source- photo by Japheth Aseko.	15
Figure 5: Mangrove forest facing threat of exploitation along Misumarini beach in Magarini Sub-County (Source- photo by Japheth Aseko.).....	17
Figure 6: The spectral curves of water, vegetation and dry bare soil at various wavelengths (adopted from Lillesand and Kiefer 2007)	23
Figure 7: (a) represent pixel vectors by their angles while (b) represent segmenting the spectral space by angle- source-(Richards, 2013).....	27
Figure 8: A flow chart showing image pre-processing, processing and post processing.....	36
Figure 9: Classified images for mto Tamamba area trend change from 1990 to 2021	39
Figure 10 : Image showing thematic change of land cover between 1990 and 2021.....	41
Figure 11 : Landsat change detection statistics (1990-2021).....	43
Figure 12: Linear regression graphs from Landsat data.....	45
Figure 13: Correlation graphs comparing relation of endmembers in Landsat data.....	47
Figure 14: Classified Sentinel-2 image showing trend of land cover change from 2015-2021	49
Figure 15: Image showing thematic change of Sentinel-2 image between 2015 and 2021	51
Figure 16: Sentinel change detection statistics (2015-2021)	53
Figure 17: Linear regression plots showing trends for endmember 2015-2021 from Sentinel data	55
Figure 18: Correlation plots for endmembers (Sentinel-2 data)	56
Figure 19: Landsat 30m resampled to 10m resolution using cubic convolution method.....	63

List of Tables

Table 1: Details of satellite data used their acquisition dates and resolution.....	31
Table 2: Landsat thematic change detection statistics.	42
Table 3: Change detection statistics for Sentinel-2 (2015-2021).....	52
Table 4: In situ- measurements collected from field campaign	57
Table 5: Confusion matrix for Landsat data	60
Table 6: Omission and Commission error for Landsat data.....	61
Table 7: Confusion matrix for Sentinel-2 data.....	61
Table 8: Omission and Commission error for Sentinel-2 data.....	61
Table 9: Confusion matrix for Sentinel-2 and Landsat 8 data.	63

List of Abbreviations

AVHRR	Advanced Very High-Resolution Radiometer
AVIRIS	Advanced Visible /Infrared Image Spectrometer
AODs	Aerosol Optical Depths
CLIND	Cloud Cover Index
DSAS	Digital Shoreline Analysis System
ENVI	Environment for Visualizing Images
EMR	Electromagnetic Radiation
ETM+	Enhanced Thematic Mapper plus
ESA	European space Agency
FAO	Food and Agricultural Organization
FLAASH	Fast Line-of-sight Atmospheric Analysis of Spectral Hypercubes
GCPs	Ground Control Points
GIS	Geographic Information System
GPS	Global Positioning System
HSR	High Spectral Resolution
ICZM	Integrated Coastal Zone Management
IOC	Intergovernmental Oceanographic Commission
IPCC	International Panel on Climate Change

MSS	Multispectral Scanner.
ML	Maximum Likelihood
NOAA	National Oceanic and Atmospheric Administration
NEMA	National Environment Management Authority
NASA	National Aeronautics and Space Administration
NDVI	Normalized Difference Vegetation Index
NIR	Near Infrared
OLI	Operational Land Imager
RS	Remote Sensing
SAVI	Soil Adjusted Vegetation Index
SAM	Spectral Angular Mapper
SNAP	Sentinel Application Platform
TM	Thematic Mapper
UNESCO	United Nation Educational, Scientific and Cultural Organization
UNEP	United Nations Environment Programme
VIS	Visible band
WMO	World Metrological Organization
WGS	World Geodetic system

CHAPTER 1. INTRODUCTION

1.1 Background

One of the most important uses of remote sensing in Earth science is the detection of changes in coastline morphology. Tidal fluctuations, waves, and longshore current are listed as among the main processes leading to shoreline changes (Mukhopadhyay et al., 2012). These processes not only play an important role in sediment budget but also modify the coastline leading to evolution. Coastline can be defined as dynamic line of boundary between land and sea (Kong et al., 2015). The change in coastline is brought about by physical as well as anthropogenic processes along the shore and has a large impact on the immediate environment and its riparian communities. Detection of coastline change plays a prime function in coastal management, risk notification, erection of coastal structures, sediment budget and shaping of coastal morphodynamics (Latella et al., 2021; Maiti and Bhattacharya, 2009)

The Kenyan coastal zone has a shoreline length that extends to over 480 kilometers between approximately 4⁰30' S and 4⁰35' N (Intergovernmental Oceanographic Commission, 1994). The area abutting the ocean provide source of livelihood to its riparian community. Structures (beach hotels) erected along the coastline are facing a major threat. Therefore, it is a crucial step to assess the pattern of soil distribution (Lobell, 2010). In addition, it is prerequisite to have detailed knowledge on the extent, nature and scale of soil erosion so as to safeguard fertile soil from being eroded. The fact that nearly half of the coastal population live along the coastal zone makes coastline dynamics due to accretion and erosion a major issue (Kevin White, 1999). Therefore, monitoring coastline evolution frequently and accurately is not only crucial in providing timely and dependable information to coastal stakeholders, but also assist in boosting the quality of studies which depend on such information for making decision. For instance, civil engineers require accurate information on coastal erosion before erecting any structure along the coastal zone. Moreover, it is necessary to have an accurate and relevant data (Coppin and Bauer, 1996) on this subject. The use of remote sensing as means of detecting coastal erosion is highly recommended since it is rapid and less expensive as compared to traditional field survey which is cumbersome and time consuming.

Many countries located to the west of Indian Ocean Kenya inclusive; have serious environmental issues related to coastal erosion. In some areas shoreline is retreating at an alarming rate (UNESCO, 1997). Since 1997, UNESCO in liaison with Kenyan researchers has conducted a pilot study on the scope and socioeconomic effects of coastal erosion in Kenya. Besides, research work related to coastal marine, coastal erosion and over-exploitation of mangrove forest near the Kenyan coast has been funded in part by the Netherlands Ministry of Development and Cooperation.

Coastal erosion is considered a threat to coastal people since it destroys coastal structures and exposes the laid buried eggs of aquatic animals to harsh environmental condition thus interfering with their life cycle. Harvard university biologist (Wilson, 2010) points out in his book, 'it is reckless to suppose that biodiversity can be diminished indefinitely without threatening the humanity itself.' Indeed, interfering with environment affects mankind severely.



Figure 1: Mangrove Forest at the beach of Bwana Saidi in Marereni Location (Magarini sub-county) source-photo by Japheth Aseko

The main factors contributing to coastline erosion and accretion include: human activities on land such as deforestation, over cultivation, clearance of land for settlement, salt harvesting, sand quarrying, poor farming methods among others. The above-mentioned factors have made coastal region very vulnerable to soil erosion in that; the top alluvial soil are swept downstream by rain water leading to sediment deposit at the shore. It should be noted that Kilifi county has over 5 salt industries located within its coastal datum. These industries rely heavily on pumped Ocean waters for desalination process. The dug trenches loosen the top soil allowing erosion to occur. On the other hand Mangrove forest which is estimated in Kenya to cover between 50,000 to 60,000 ha at the coast; faces big threat due to non-sustainable utilization and over exploitation (Kairo, 1995). Figure 1 above shows network of mangrove roots along the Kenyan coastline. Reduction in mangrove forest impact negatively on surrounding economy as indicated by decrease of fishery resources, firewood shortage, demolition of corals, exposes human settlement to wave impacts and

exposes bare surface to erosion agents. Coastal erosion is a serious threat, because the loss of fertile soil is often accompanied by decrease in food production. The current existing methods of identifying the affected areas are based on physical survey, which of course are more expensive and time consuming. It is therefore more appropriate to use more sophisticated method of getting information and remote sensing via the satellite data offers an effective remedy.

This study aims at monitoring coastal erosion and accretion along the Kenyan coastline using satellite images (Landsat and Sentinel-2). The images were downloaded for free from various websites (USGS, ESA and earthexplorer) from 1990 to 2021. To achieve this objective, images acquired at different time interval were classified separately and thematic change detection techniques used in assessing the impact of erosion. The susceptible areas were mask out using image subset technique and the time series trend of bare land, water and vegetation analyzed using Excel software.

1.2 Statement of research Problem.

Kenyan coastline has evolved overtime. Erosion and accretion are the root causes of this evolution. This change in coastline morphology poses serious threat to marine ecosystem, recreational facilities, infrastructure development, tourism industry, food security among others. The Knowledge of coastline dynamic is important both to coastal developers, county government and National government who erect structures within and along the coastline. A time series monitoring of this evolution is required to assess its spatial extent and predict its future impact. This research seeks to use images from satellite to establish the extent of change in coastline morphology.

The mangrove forests which provide a line of defense against shoreline erosion has since been encroached thereby giving room for coastal erosion. The reduction of mangrove population along the coastline makes the surface along the coastal boundaries more vulnerable to coastal erosion. To make matters worse the oceanic tide and waves find ways on bare coastline and erode it with ease. This does not only interfere with breeding ground of marine ecosystem but also their life cycle.

The effect of global warming has resulted into sea level rise; this implies that a portion of land that is adjacent to the ocean has either been eroded into the ocean or flooded. These gradual sediments

deposit has led to change in coastline morphology. This requires frequent monitoring to predict future advancement of this menace.

Many research on soil erosion has been done at the Kenyan coast however, they are based on old traditional survey methods which are labor intensive, time consuming and uneconomical. Therefore, use of satellite sensors (e.g Sentinel-2, Landsat) data as way of monitoring this menace is the most appropriate since this method is cheap, reliable, cost effective and easy to retrieve if need be.

This research will provide a diverse array of data that will lead to an in-depth mechanistic hypothesis that will inform reserve management of this region on real picture on the ground. In a nut shell, it will not only assist coastal zone management in making sound decision on this matter but also other stakeholders such as environmental research bodies.

1.3 General Objective

This study aims at monitoring coastal erosion and accretion using satellite images (Landsat, Sentinel-2).

1.3.1 Specific objective

1. To acquire the relevant satellite datasets from Sentinel-2 and Landsat satellite for the period of interest and classify predominant features in the image using maximum Likelihood image classification techniques.
2. To use ENVI and ArcGIS software to analyze and ascertain the impact of coastline evolution in the susceptible area using thematic change technique.
3. To obtain temporal (time series) and spatial variation statistics of endmembers and find correlation between various land cover types.
4. To validate resampled classified Landsat data using high spatial resolution Sentinel-2 image.

1.3.2 Hypothesis

Deforestation, quarrying, salt manufacturing and human encroachment on public land are well known factors contributing to evolution of shorelines in any coastal region. Is it possible that some section of Ocean waters has receded into the land? If so to what extent? Climate change due to global warming has led to rise in sea level thereby increasing hydrodynamic effects along the coastline leading to coastal retreat and accretion. Ocean water dynamics are known to erode sea bed sediments to the shore: Do this eroded sediments have any impact on coastline? Can spatial extend of this menace be monitored using satellite data? What effect if any, does erosion have on marine ecosystem and its riparian community? Is it possible to predict future impact of erosion using satellite data? It is expected that the synoptic capability of satellite sensor in monitoring land surface change at different scale, will provide a cheaper alternative to the old traditional method of monitoring coastline evolution.

1.4 Justification and Significance

Coastal erosion and accretion leads to coastline shift. The drivers of shoreline dynamics include: unplanned and unregulated beach front development, poor agricultural practice, overexploitation of resources, the action of oceanic tides along the coastal strip, and the consequences of Sea level rise.(Kimani et al., 2017).Coastal erosion have adverse effects on food security , marine ecosystem, hinders navigation of ships and destroys recreational facilities. Fishing industry, tourism and riparian community faces a major threat if this menace is inadequately addressed. To effectively control this menace reliable and timely information on state and rate of coastline change is prerequisite. The old methods of monitoring erosion via field survey is time consuming and uneconomical. This study adopts RS and GIS monitoring techniques to assess effects of erosion and accretion along Kenyan coastline. Analysis methods like time series and thematic change techniques have aided in identification and assessment of its impact. The fact that little has been done in this part of Kenya using RS on the subject, was a motivating factor towards this work. This work will aid stake holders in making sound decision regarding the state of coastal erosion and take prompt control measures.

1.5 Area of study

Coastal strip is a region within coastal region of Kenya just adjacent to the shore of Indian Ocean. The Kenyan coastal zone extends from about 4°30' S to 4° 35'N and has a total shoreline length of over 480 km (<https://www.naturalworldsafaris.com/africa/kenya/kenyan-coast>). The region from sea level datum to about 200m is called coastal plain and is considered as the most affected by coastal erosion since most activities at the coast take place here. In other words, massive investments of national importance are situated in these areas which are susceptible to erosion. Kenyan coast is inhabited by Arabs, Mijikenda, Akamba, Swahili people among others. According to Kenya-census (2019) this coastal region does not only cover an area of 79,689 km² but also has a population of 4,329,474. This study focuses on the coastal strip.

Kenyan coastal climate is tropical humid and is influenced by the monsoon wind which is characterized by two distinct rainy seasons. Long rainy season is between March to May and coincides with south-east monsoon wind whereas short rains which is from October to December corresponds to northeast monsoon wind (Camberlin and Planchon, 1997). Annual average rainfall along the coast varies from 500-900mm per year on north coast to 1500-1600 mm per year on south coast. The mean minimum and maximum temperature at Kenyan coast range between 24°C and 30°C.

Coastal counties are endowed with natural resources which act as attractive sites for tourists. Among these resources is mangrove forest (Arabuko forests) which has since been invaded by coastal people in search of timber, medicinal plants, and some portion cleared for agriculture. Besides agriculture, other economic activities include; fishing, salt harvesting, trading, beekeeping, quarrying and tourism. It is feared that if the trend of forest encroachment continues there will be reduction of forest cover, loss of biodiversity and increase in soil erosion which will impact negatively on livelihoods of coastal people. Generally, anthropogenic pressure has brought about the degradation of coastal resources putting the livelihood of riparian communities in

jeopardy. For instance, poor land practices upstream and deforestation leads to immense sedimentation downstream, impacting negatively on coral mangrove and other ecosystem (Kitheka *et al.*, 2005). These massive sedimentation has led to shore line retreat and accretion. This study focuses on monitoring the effect of sediment deposit on the coastline. Due to challenge of clouds, only areas susceptible to tangible change within the coastline was focused on.

This study identifies Mto Tamamba delta in Marereni location along the coastline as the most affected area. Mto Tamamba region extents from about $2^{\circ}45'$ S to $2^{\circ}48'$ S and has a total shoreline length of approximately 3.8 km. It borders Tana river to its North, Kanangoni township to the West, Marereni township to the South and Indian Ocean to the East. Mto Tamamba is located in Marereni location, Magarini Sub-County in Kilifi county. This sub-county is a host to many salt manufacturing industries that supply salts to entire Republic of Kenya. The study area is approximately 12 square Kilometers. The natives are mainly Mijikenda whose economic activity include fishing, coconut farming, goat rearing and trade. In order to avoid massive clouds which is a characteristic of coastal region, this region was masked out for further scrutiny. The figure 2 below shows location of Mto Tamamba area.

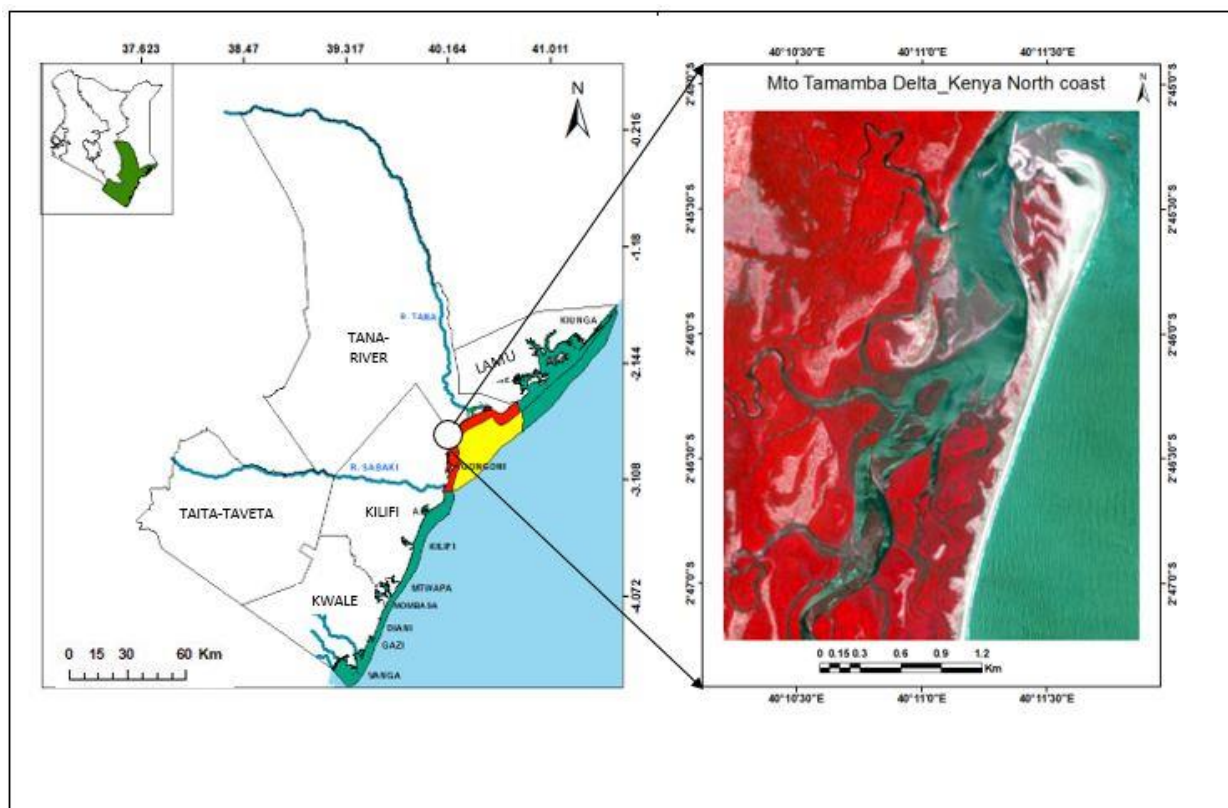


Figure 2: Map showing RGB image of study area (Mto Tamamba) encircled (Adapted from (Latawiec and Agol, 2015) , KMFRI).

CHAPTER 2. LITERATURE REVIEW

2.1 Remote sensing technology and application techniques

2.1.1 Developments in Remote Sensing Technologies

Remote sensing (RS) refers to the process of detecting and monitoring the physical characteristics of an area by measuring its reflected and emitted radiation at a distance (typically from satellite or aircraft). The innovation of camera over 150 years ago led to the foundation of the current RS technology. Cameras were mounted to tethered balloons for topographic mapping in the 1840s; the concept of earth's surface observation emerged at that time (Famiglietti et al., 1999). During the First World War, military explored the earth's surface by mounting installed cameras on aircraft. By 1950s Ms. Evelyn of US Office of Naval Research defined remote sensing as the art of finding, viewing and measuring an object without being in direct contact with it (Famiglietti et al., 1999). Even though this was viewed as an achievement in the then years but it lacked proper data storage skills.

With technological advancement, computers could convert analog data to digital format, store and retrieve such data. The social movements of the 1960s and 1970s raised public awareness of the physical environmental changes that were explored and augmented by computers, enabling their detection, monitoring, and analysis with the aid of satellite remote sensing photography. As time went by, many sensors were invented. These sensors could concurrently record the earth's surface in various locations on the planet utilizing various electromagnetic spectrum bands. The first satellite launched by Landsat in 1972 was Corona, a project run by Earth Resources Technology Satellite (ERTS). Nowadays, many satellites are equipped with different remote sensing gadgets that enable them take, record, send and save high resolution imagery. Such images enable scientists detect changes on Earth's surface. Remote sensing explores the advantage that each and every object has unique spectral characteristics that can be identified by sensors.

The acquisition of RS data involves mounting of sensors on satellites evolving around the earth, which take information about surface objects by detecting energy reflected from them. These Satellite have inbuilt optical advanced Charge Couple Devices (CCDs) instruments capable of taking images and converting them into electronic signals which are then channeled to ground station. Figure 3 shows how images are captured using Satellite.

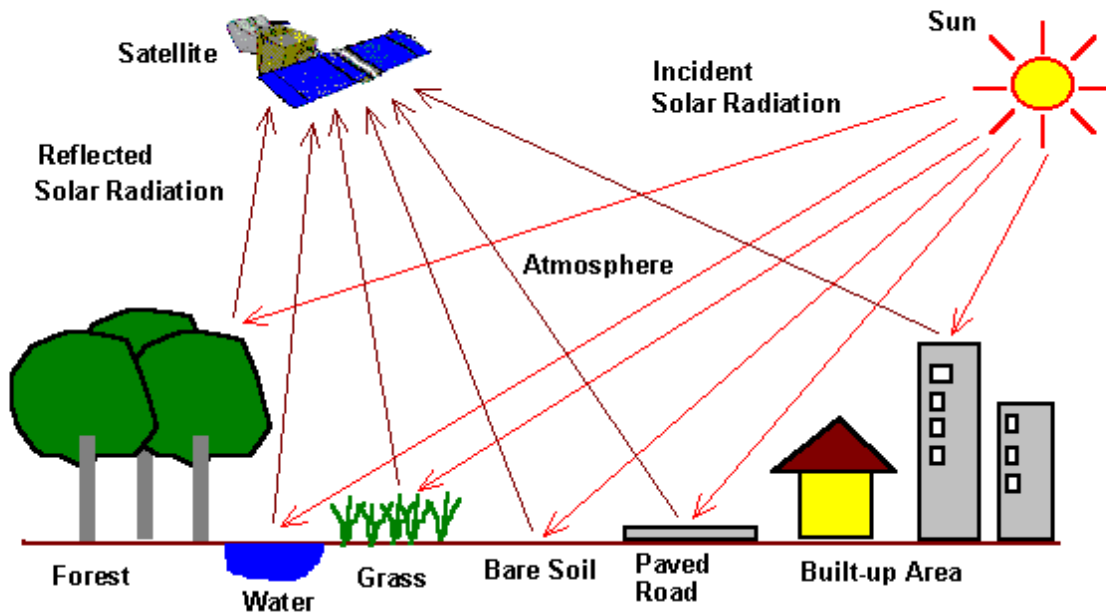


Figure 3: Reflected Solar radiation being detected by satellite. (source – <https://www.crisp.nus.edu.sg>).

RS has wide applications which includes: Management of natural resource which is aimed at protecting natural resources; Hazards assessment (floods, erosion and hurricane tracking); coastal application (Monitoring shifting shorelines and Sediment transport) among others. This study explores the use of R.S in coastal application.

2.1.2 Shoreline Extraction and Change Detection

The fact that not much has been done in Kenya in connection to coastline erosion and accretion spearheaded our urge to use satellite images to monitor the extent of this menace. Many researchers worldwide have used several methods in assessing coastal vulnerability. This includes remote sensing, geographical information system, dynamic assessment tools and vulnerability indices

among others (Chaib et al., 2020). Coastline vulnerability is defined as the potential for natural hazards on the coast to inflict damage (Burton et al., 2005). Changes in the global climate have increased the frequency of natural disasters such as storm surges, tsunamis, and cyclones, wreaking havoc on coastlines (Leone et al., 2011). The tsunami of December 2004 and the thane cyclone of 2011 both wreaked havoc on the coastlines of Puducherry and Tamil Nadu, causing massive human and economic losses (Mani Murali et al., 2013). The destruction created by the aforementioned catastrophes necessitates vulnerability assessment in order to identify the factors that cause the menace. On a global scale, the most often utilized methods in the research of coastal erosion and accretion are remote sensing (RS) and geographic information systems (GIS). For example, (Saravanan et al., 2014) used RS and GIS to manage coastal erosion in Southeast India. (Wang et al., 2013) used six remote sensing images to determine shoreline change in China's Pearl River Estuary from 1986 to 2011. (White and El Asmar, 1999) employed a variety of satellite images, including MSS, TM, and ETM+, to determine coastline erosion. Rosetta promontory lost 113.8 m per year between 1984 and 1991 (Elsayed and Mahmoud, 2007). Shoreline Erosion Hazard in Microtidal coastal environment (Italy) was evaluated with VHR optical data set along the Mediterranean sea (Cenci et al., 2021). The long-term shoreline oscillation in Cauvery Delta at Poompuhar, Tharangambadi, and Nagapattinam was studied using satellite images (Sridhar et al., 2009). Coastline change in the Aksehir and Eber lakes in southwest Turkey was determine using different remote-sensing methods on satellite images. (Şener et al., 2010). Along the Turkish coast of black sea shoreline changes was detected by (Kuleli et al., 2011).

The Kenyan coast, like other coastlines across the world, has been subjected to natural and human-caused coastline erosion and accretion. Many research work on coastal erosion in this region are based on field survey. Erosion related to unwise agricultural practice, clearance of land for settlement, dredging of seabed and deforestation are prevalent at the Kenyan coast (Odada, 2001). Because the loss of fertile soil is generally followed by a drop in food production, coastal erosion is a severe problem. Physical surveys, which are of course, more expensive and time demanding, are currently used to identify the afflicted areas. As a result, this study explores the use of more acceptable and less complex methods of gathering data, and satellite remote sensing provides an

effective remedy. Research work done by (Johnson, 2013) along the coastline reveals that, Malindi Bay receives high terrigenous sediment load amounting to $5.7 \times 10^6 \text{ ton} \cdot \text{yr}^{-1}$. Coastal erosion and sedimentation carried by River Sabaki affect not only the beaches but also the coral of Malindi area (Hoorweg and Muthiga, 2009). Coastal erosion is severe in a number of sandy beach areas such as North and South of Mombasa and Malindi – Mamburui area, while in areas around Mamburui village, rapid accretion is occurring (KMFRI, 2003). Before 1976 Malindi was experiencing loss of land, but from 1976 to date, the beach at Malindi has prograded by about 500m (Omuombo et al., 2013). Coastal erosion is also prevalent along the cliffs beaches at Kanamai, Shanzu, Ivwetine, Nyali, Likoni, Black Cliff Point, and Tiwi (Abuodha and Kairo, 2001).

The goal of this study is to use satellite images (Landsat and Sentinel-2) to track the impact of erosion on Kenya's coastline. Remote sensors via satellite have the capability of monitoring land surface changes and degradation on different scales. The ability of satellite sensors to distinguish spectral signature of various elements (water, soil, vegetation) has made it possible to accomplish the objective of this research. This work combines RS and GIS approaches to monitor silt distribution along the Mto Tamamba delta (from 1990 to 2021) and provides conclusions based on time series data. This study was motivated by the evident need to control the threat of coastal erosion to coastal communities in Kenya and the whole world.

2.1.3 Shoreline Mapping Techniques

A variety of methods have been developed by scientists to map shorelines. Historically, scientists have mapped shorelines using ground survey techniques (Li and Damen, 2010). This was done by using a plane table and a rod to measure the direction and length of the beach (Graham et al., 2003; Liu, 2009). In the 1920s, aerial photography replaced the conventional technique of shoreline monitoring. Cameras installed on aircraft took aerial photographs, and changes in the shoreline could be seen by comparing images collected over time (Graham et al., 2003; Liu, 2009). Aerial photographs that have been spatially referenced are made available via the GPS, enabling users to determine the location of shorelines with accuracy (NOAA 2014).

Another way for mapping shorelines is to use kinematic differential GPS on top of a four-wheel-drive vehicle; the vehicle can drive at a steady speed along a shoreline of interest (Morton et al., 1995). In general, this strategy is very accurate, low-cost, and quick at gathering information

(Morton and Speed, 1998). However, the precision is dependent on the GPS device's spatial accuracy.

Presently, it is possible to map the shoreline using satellite images and high-quality data however, this depends on the spatial resolution (Klemas, 2010). This method has merits over other methods since it has a wide field of view that capture wide area at once and a spectrum capacity which makes it possible to distinguish between land and water features using infrared bands collected by the sensors (Alesheikh et al., 2007). Landsat data is one type of satellite image data that is freely accessible; other types of satellite image data (high spatial resolution) are acquired from organizations like IKONOS, Quickbird, and Worldview at a cost. To accurately detect coastline changes, high spatial resolution data is preferable (Klemas, 2010). However, such data may be expensive.

Light detection and range (LIDAR) mapping is the most advanced and accurate method for mapping shorelines. In this method, the laser beams journey time is calculated from the moment it leaves the device until it returns following reflection (Lobell et al., 2010). With respect to x, y, and z coordinates, it gathers three-dimensional points. Unlike aerial photographs and satellite images, LIDAR enables researchers to gauge volume changes. Despite being expensive, it swiftly covers large areas, making it the method of choice (Boak and Turner, 2005).

2.2 Coastal Environmental issues.

2.2.1 Coastal erosion and accretion.

The natural occurrence of coastal erosion along the world's coastline is caused by the movement of currents and waves, which causes sediment loss in certain areas and accretion in others (Fan et al., 2017). Accretion is the gradual accumulation of sediments to form layers. This gradual accretion and erosion of sediment results into evolution of coastline. The initial coastal maps were developed based on early boundary of land and water. However, with gradual piling of sediments it is no doubt that these boundaries have since been displaced. In most cases coastline evolution is caused by water waves that are generated by storms, wind or first moving motor craft. The overharvesting of timber and poles for building houses and boats and the burning of charcoal as well as harvesting medicinal plants from mangrove forest (Abuodha and Kairo, 2001) has also contributed a great deal to this menace. According to IOC report (1994), the work of Kenya coastal

erosion monitoring began in 1987; however, they were based on field survey. In this report it was realized that the best way of monitoring coastline evolution was on long-term basis and satellite data offered the best alternative. Coastal erosion can either occur due to man's activity on land or as result of action of sea water on the coastline. Figure 4 below shows effect of coastal erosion on the beach of Bwana Saidi in Kilifi county (Kenya)



Figure 4: A section of piled eroded sediments from the ocean along the shores of Bwana Saidi beach in Magarini Sub-County (Kilifi County).-Source- photo by Japheth Aseko.

Along the shoreline the dynamic process that exists is generated under the influence of fluid motion which manifest itself as coastal currents, tidal currents, surface waves, storm surge, tsunamis and others (Carter and Woodroffe, 1997). Findings from field survey in this area identifies human influenced activities such as exploitation of mangrove at the edge of forest (Shirazi-Funzi lagoon),

that uncovers the shoreline allowing wave current to erode the exposed area (Munyao, 1993). Figure 5 below shows the cutting of mangrove trees for charcoal burning in Misumarini beach. In fact, (Odada, 1993) points out clearly that erosion linked to imprudent agricultural practice and tree logging is frequent at the Kenyan coast. Moreover, he adds that Coastal erosion is mainly caused by poor agricultural practice, clearance of land for settlement and deforestation. Development of ports and harbors, coastal construction such as reclamation of land for airport construction and dredging of seabed also cause coastal erosion and especially siltation (Odada, 2010). Another factor contributing to coastal erosion is population pressure which leads to subsequent increase in food demand and thereby shrinking the available land for agriculture because the same land is used for accommodation, industry, road expansion, playing field among others and hence leading to over cultivation. In reality, with rapid increase in population the overall net land resources available for agriculture is bound to decline. Other effects of coastal erosion include, erosion of agricultural pesticides into the Ocean thereby impacting on marine ecosystem.



Figure 5: Mangrove forest facing threat of exploitation along Misumarini beach in Magarini Sub-County (Source- photo by Japheth Aseko.)

A part from the natural processes, human activities such as sand mining, dredging and vegetation clearance tends to accelerate this menace. Sand harvesting does not only interfere with natural replenishment of beach sand but also destroys nesting area for turtle. Shoreline erosion poses a constant threat to infrastructure (Beach hotels), leading to expensive engineering coastal protection measures. It should be noted that tourism in particular, depends on a healthy environment and a rich biodiversity: so with deforestation and coral reefs degradation the near shore fish productivity declines hence making soil erosion a serious threat both to national and local economy. Not only does Retreat in the coastline cause hazards by uprooting settlement, destroying agricultural land, disrupting harbor and navigation structures but also dislodge valuable commercial facilities

situated along the shoreline (Odada, 2001). Natural factors connected to this menace include; landscape orientation, tidal fluctuation, stormy wave regime, and rise in sea level among others.

2.2.2 Sea level rise.

African coastal regions along the shoreline of Indian and Atlantic Oceans have increasingly been exposed to the effects of climate change, including sea level rise (Leatherman et al., 2000). Moreover, the coastline of the eastern Africa sub-region which Kenya is a party has been receding inwards and seawards due to Sea level fluctuation; an aftermath of climate change. (Odada, 2010).

One of the most visible effects of climate change is accelerated sea level rise. Sea level increases at a rate of 1.3 mm per year along Indian coasts (Church et al., 2013). Rising sea levels wreak havoc on the coast, causing a plethora of erosional hazards. The depth of the water, as well as the depth of the wave base increases as the sea level rises. As a result, the water level begins to rise along the coast. Consequently, low African coastal areas recede inwards by a few hundreds of meters jeopardizing the construction of proposed coastal structures (Church et al., 2013). As the waves reach the shoreline, their intensity increases, allowing them to erode and transport more sediment. Tidal waves, storm surges, and flooding are all enhanced by rising sea levels. These effects are not only harmful to coastal ecosystems (mangroves, turtles that deposit their eggs on the sand) but also to coastal infrastructures.

Flooding could endanger lives, livestock, agriculture, infrastructures and buildings. It is worth noting that rise and fall of sea level will definitely lead to change in coastline. This change will have an impact on existing coastal maps. With global warming in place sea level is definitely bound to rise; hence calling for anticipatory planning and action to avoid chaos. To arrest this, rapid and frequent monitoring of coastline retreat is vital and remote sensing satellite data offers an effective remedy.

Use of remotely sensed data to monitor coastal retreat will provide information on continuous change in landscape. Past images of more than three decades ago can be downloaded and comparison made with the current ones to monitor coastal retreat. The result obtained will enable

stakeholders formulate policies to address this menace. However, it should be noted that the main challenge in monitoring coastal retreat is the concept of ‘sediment budget’ which is concerned with replenishment and withdrawal of sediments at the shore. However, it is believed that an interval of thirty years between the image data will provide a significant change detection needed for this study.

2.2.3 Desalination Process.

Desalination is the process of extracting salt from salty Ocean waters. The coastline of Magarini Sub-County in Kilifi county host majority of salt industries at the coast and these factories do not only depend on Ocean water as raw material but also pump these salty waters to the land adjacent to the shoreline. This desalinization process has impacted negatively on riparian communities. Ground truthing exercise conducted confirms displaced population inlands with their agricultural and grazing land occupied by dug salty water basins. These water basins are filled by ocean water on daily basis. The few residents remaining are leaving in fear lest they be evicted. Most of their land adjacent to the ocean had been leased to salt factory owners since 1975. The vast land which were occupied by mango and coconut plantation have currently saving as basins for salty waters for these factories. These plantations which held the soil fabric together are no longer there, hence top soil are easily eroded to the banks of rivers and Ocean. The natives of Marereni and Kanangoni are languishing in poverty because their source of livelihood (mangoes and coconut) are facing extinction. It is expected that this continuous diversion of this natural resource will lead to reduction in level of Ocean water which will eventually have impact on coastline geomorphology. This study aims at monitoring the effects of both natural and human activities on the coastline.

CHAPTER 3. THEORETICAL BACKGROUND

3.1 Change detection techniques

The process of observing and identifying differences of state of an object at different time interval is called change detection (Singh, 1989). Comprehending the relationship and interaction between human and nature for better decision-making, requires timely and precise change detection of earth's surface features (Lu et al., 2004). The change detection enables us understand dynamic change of landscape.

Quality change detection entails; geographical distribution of change kinds, change rate, change trajectories of land cover types, area change and accuracy evaluation of change detection results. Change detection is aimed at comparing representation of two points through time and space by suppressing all variances causing variable difference and controlling unwanted variables (Kempka and Lackey, 2012.). The fundamental assumptions underlying the use of remotely sensed data for detection of change is that; change of the object of interest will result into corresponding change of reflectance value of that distinct object. It should however be noted that variation factors like illumination angle, cloud cover, atmospheric conditions and soil moisture may have pronounced effect on the final image; calling for image preprocessing procedure.

The three key components of change detection in resource monitoring are; identifying the nature of change, detecting if change has occurred and computing area extent of the changes (Macleod and Congalton, 1998). Technological advancement has made the subject of earth surface monitoring vital thereby making researchers develop new change detection techniques. In this study we use thematic change detection technique in ENVI 5.3 platform to track Kenya's coastline evolution history.

3.1.1 Image differencing

This change detection method is preferred mostly by researchers due to its' easy implementation and interpretation. This method involves subtracting digital values of pixel of a given image from those of the corresponding pixels of an earlier image. The resulting dataset shows positive values in areas where the digital values have increased over time whereas those regions where the digital

values have decreased over time will have negative values (Jensen, 1996). Zero values could imply no change. However, it should be noted that this technique lacks provision for matrices of change information. In addition, challenge in selection of suitable threshold for identification of changed region is its big demerit.

3.1.2 Clouds and cloud shade removal

Remotely sensed images collected from coastal region and mountains often have clouds as common features in their visible and infrared bands. These clouds contamination cause serious missing data due to blockage of underlying features; hence limiting application of such data. To address this challenge, cloud should be masked out and their position be replaced by data from a “reference image”. However, availability of a totally cloud-free “reference images” in coastal area is rarely realized. This is worse especially in Landsat data which has a repeated coverage period of about sixteen days.

Thick clouds have shades covering land features more so if sensor is not at nadir when taking images. These cloud shades block clear visibility of land surface. Both clouds and clouds shade need to be masked out as preprocessing procedure. However, such removal if done on images of high percentage cloud cover, the quality of the processed image is compromised. This calls for setting cloud percentage threshold below which data shall be considered valid. In this work we set a threshold percentage cloud cover of below 5%. The ENVI 5.3 software applies various band math equation in masking of clouds. This process involves setting thermal variation that enable identification of clouds and their shades.

3.2 Object Detection and Discrimination

The process of object identification depends on incident radiation from the sun. This radiation when directed on the Earth's surface can either be absorbed, transmitted by or emitted by the surface (Lillesand et al., 2015). The interaction of EMR is represented by equation 1.

$$E_i(\lambda) = E_R(\lambda) + E_A(\lambda) + E_T(\lambda) \quad (1)$$

Where $E_i(\lambda)$ = incident energy

$E_R(\lambda)$ = reflected energy

$E_A(\lambda)$ = absorbed energy

$E_T(\lambda)$ = transmitted energy

Generally, the basis of identification of objects relies on the fact that each object emits unique radiation energy when illuminated by sun. In addition, energy emitted from distinct objects can be analyzed for purpose of discrimination (Sivakumar *et al.*, 2003). It is important to note that spectral reflectance curves for these features are very distinct from one another. In other words, the nature of the curve depicts the condition and type of object it applies. The spectral reflectance curve for water, soil, and plant is depicted in Figure 6. The reflectance characteristics of earth surface features are expressed by equation 2:

$$\rho(\lambda) = [E_g(\lambda)/E_i(\lambda)] \times 100 \quad (2)$$

Where $\rho(\lambda)$ = Reflectivity

$E_g(\lambda)$ = Wavelength energy reflected from object

$E_i(\lambda)$ = Incident energy on the body

It is worth noting that some conditions, such as plant health and plant size, climatic condition can cause variation in these reflectance curve. In plants the internal structure of leaves has chlorophyll that absorbs strongly electromagnetic radiation (EMR) in the visible light (VIS) and reflects strongly in near-infrared (NIR) part of the spectrum. In contrast to plants, some aspects of soil reflectance include; organic matter content, soil texture, surface roughness and moisture content. These elements are intricate, varied, and interconnected. For instance, soil reflectance will decrease when it is moist and vice versa. On the other hand, coarse sandy soil has a pretty good

drainage system, which results in low moisture content and a high reflectivity (Lillesand et al., 2015).

Water differs from other features in that it has ability of absorbing EMR and NIR wavelengths and beyond. It is important to keep in mind that; the reflectance curve of water body is not a function of water only but also components in it. For instance, water with significant large amounts of suspended particles from soil erosion typically has a substantially higher apparent reflectance than clean water. Plants with high concentrated chlorophyll content tend to have an enhanced green wavelength of water reflection and decreased the blue wavelength reflectance. Through the use of RS data, these characteristics have been used to track land cover changes.

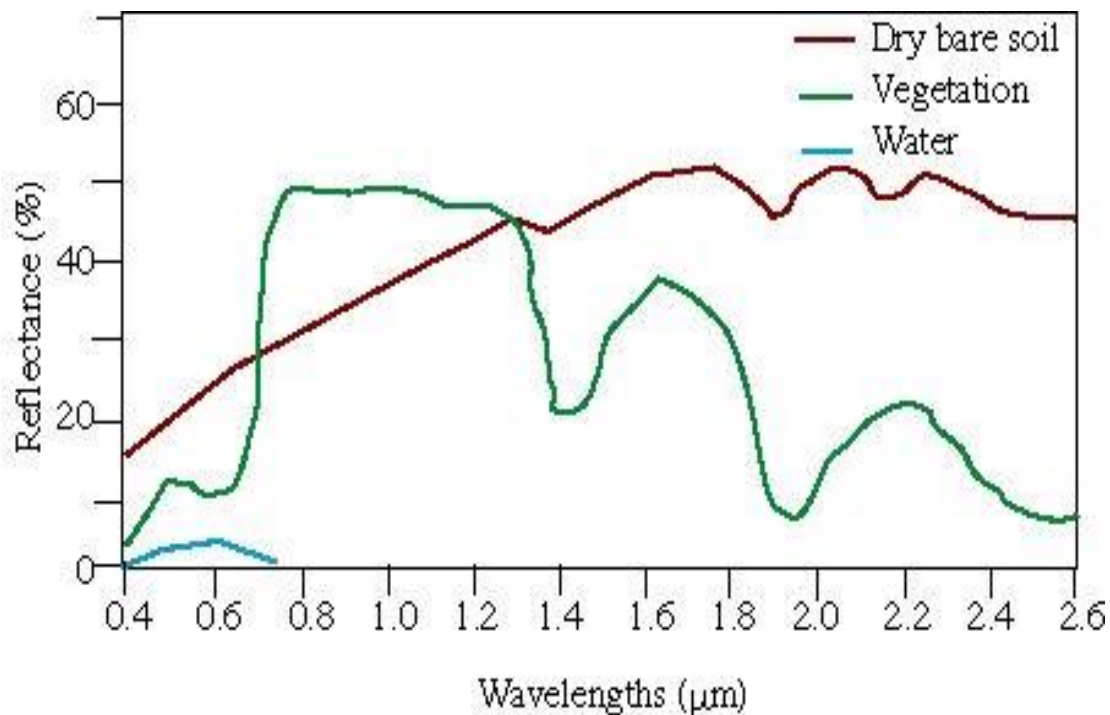


Figure 6: The spectral curves of water, vegetation and dry bare soil at various wavelengths (adopted from Lillesand and Kiefer 2007)

3.3 Vegetation Indices

Vegetation indices are the combination of surface reflectance of at least two or more wavelengths; particularly designed to emphasize the vegetation property. They are acquired relative properties of vegetation. Reflectance in leaves is greatly influenced by pigment concentration on the leaves,

the broadness or narrowness of the leaves, the canopy formed by such leaves and the health of the plant. Generally, plants absorb highly in VIS part of electromagnetic radiation (EMR) implying that the reflectance of leaf at this region is very low. On the other hand, plants reflect EMR highly in NIR portion. There are many vegetation indices in place but this research shall focus on NDVI. NDVI has been chosen in this work for the purpose of monitoring mangrove forest.

3.3.1 Normalized Difference Vegetation Index (NDVI)

The normalized difference vegetation index (NDVI) is a straightforward numerical indicator that analyzes remote sensing measurements to determine whether the target under observation contains live, green vegetation or not. It uses the visible (RED) and near-infrared (NIR) portions of the electromagnetic spectrum. The NDVI is entrenched on the fact that solar radiation is absorbed and reflected by green vegetation.

In vegetative studies, NDVI has a wide range of uses including; estimation of forest cover, pasture performance, crop yields, rangeland among others. It frequently correlates to; ground parameters like biomass concentration, surface water, plant water content, leaf area index (LAI), and photosynthetic activity of the plant.

In general, a healthy plant will reflect most of the near-infrared light that strikes it and absorb most of the visible light and vice versa. Conversely, barren land reflects modestly in the electromagnetic spectrum: red and near-infrared regions (Engvall et al., 1977).

The NDVI algorithm subtracts the RED reflectance values from the NIR values and then divides it by the sum of near-infrared and the red bands. See equation 3.

$$NDVI = \left(\frac{\beta_2 - \beta_1}{\beta_2 + \beta_1} \right) \quad (3)$$

Where β_1 is red band and β_2 is near-infrared band.

The formula above enables us to justify the likelihood of two alike vegetation blotches having different NDVI values depending on environmental location or difference in degree of exposure

to sunlight. The bright pixels would have larger values and a greater absolute difference between the bands.

NDVI values ranges from -1 to 1. The values closer to negative or negative represents water or clouds, bare land values cluster around zero while closer to 1 depicts dense vegetation preferably forest.

3.4 Types of classification

The process of making significant digital thematic map out of an image data set is called image classification. In most cases, classification is carried out using multispectral data; the spectral pattern existing inside the data serves as the numerical basis for classification (Lillesand et al., 2015). Similar pixels are categorized into endmembers which are extracted by algorithms or from familiar cover types. Computer algorithm partitions the image into sections that match each land cover type; with data specific values from the various cover types in the image known. A single image data set or numerous images taken at various times can be used for classification of image. The aim of this classification is identification and depiction of unique gray level (or colors) of features appearing in the image in terms of objects or types of land cover.

There are two types of classification algorithms namely; unsupervised and supervised classification. In both methods the region enveloped by each category of pixel is displayed on the culminating thematic image. When converting pixel into thematic map, unique endmember types are categorized either by analyst or computer clustering algorithms. The pixels in the image are grouped into spectrally distinct units during clustering. These can then be utilized to define a set of spectrally distinct signatures or used directly as a categorized image. In contrast, the analyst approach uses the sample pixels to determine the identity of each cover type. Upon the definition of signatures, decision rule algorithm places each image pixel in one of the cover type classes.

3.4.1 Supervised Classification

In this approach the identification of pixels of known cover type is done by the analyst before the computer algorithm is allowed to batch other pixels into prior analyst identified categories. The primary tool used in drawing out quantifiable information from remotely sensed image data is called supervised classification (Richards, 2013). By using this technique, the analyst can construct

representative parameters for each class of interest using a sufficient number of known pixels. Three key steps involved in this process are; pixel training, classification and output. The users' goal is to generate "seeds" meant for classification thereafter. The classifier is then used to assign labels to all image pixels in accordance with the trained parameters.

3.4.1.1 Data training

For effective supervised classification proper data training is prerequisite. The training "seeds" can either be picked by the analyst from the region of study or from the image. Familiarity with the study area through google earth or by prior visit leads to an effective data training. During this process each image pixel is assigned to land cover type that it most closely resembles. In the contrary, pixels that do not conform with trained parameters are branded unclassified. Supervised classification algorithms include; maximum likelihood, parallelepiped, spectral angular mapper, minimum distance just to mention a few. The algorithms use in this study are discussed as under.

3.4.1.2 Maximum likelihood

Maximum likelihood (ML) algorithm applies discriminant function in assigning each pixel in the region of interest to class of the most probable land cover type (**Ahmad and Quegan, 2012**). The function primarily inputs, the class mean vector and covariance matrix which can be calculated from the training pixels for a given class. The classification process involves choosing a specific threshold and file location for the data. If the probability values fall below the user-specified threshold, each pixel is either categorized into the class of the highest likelihood or otherwise marked as unclassified (**Ondieki et al., 2022**). Bayes theorem states that, for a posteriori $P(i|\omega)$, the probability that a pixel with feature vector ω belongs to a class i is given by equation 4

$$P(i|\omega) = \frac{P(\omega|i)P(i)}{P(\omega)} \quad (4)$$

Where $P(\omega|i)$, is the likelihood function, $P(i)$ is the a priori information, i.e, probability that class i occurs in the area of study and $P(\omega)$ is the probability that ω is observed.

The ML algorithm puts into account the following steps; determines total number of land cover types then selects the training pixels for each class. Lastly, each and every pixel in the region of interest is either categorized into land cover types or otherwise branded unclassified.

3.4.1.3 Spectral angular mapper

Spectral Angular Mapper (SAM) divides the spectral domain on the base of vectors measured from the origin, as illustrated in two dimensions. Figure 7 shows domains of SAM.

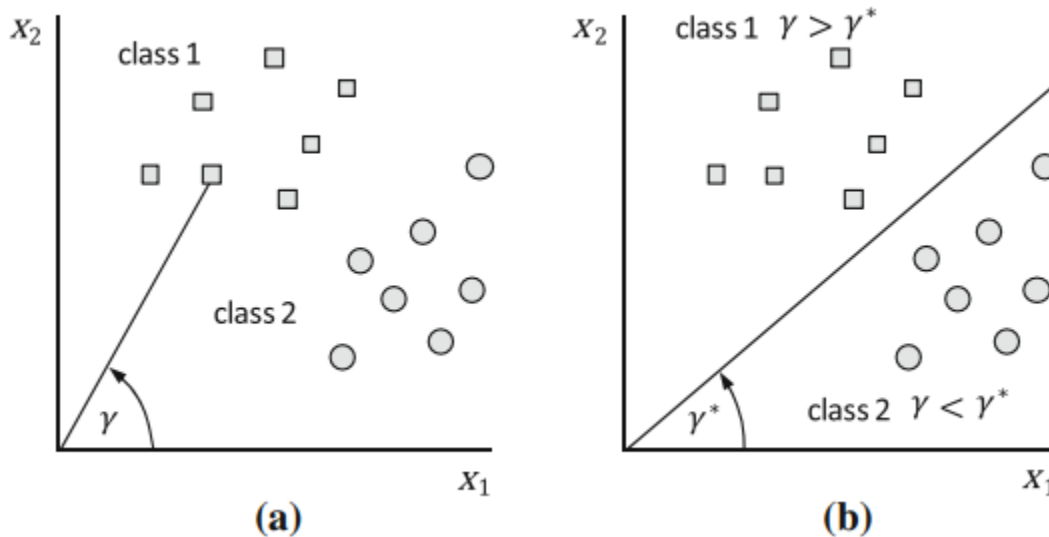


Figure 7: (a) represent pixel vectors by their angles while (b) represent segmenting the spectral space by angle- source-(Richards, 2013)

SAM is based on the idea that every pixel point in spectral space, when written in polar form as opposed to the more common Cartesian form, has both a magnitude and an angular orientation. The distinction between trained pixels in various classes is represented by the dimension boundary shown above. The fundamental benefit of the SAM approach is that endmember spectra extracted from an image in one year can be used to classify images in consecutive years as long as equal number of bands are maintained: this ensures consistency in the classification process.

3.4.2 Unsupervised classification

Under this technique the computer algorithm randomly generates definite cluster points in data space which are elucidated by the analyst as various cover kinds. In other words, the all pixels in the image are randomly arranged into several classes by this algorithm based on inherent assembling found on image values. The fundamental premise is that data belonging to the same class should be relatively well separated, whereas values belonging to a particular cover type should be bundled together in the multi-dimensional spectral space. The resulting classified image contains unknown cover types which are then corded by analyst into spectral classes based on some reference image or pictures of the region of interest.

3.5 Image enhancement

This procedure involves removing undesired elements from a row image to enhance its aesthetic effect. Increasing the radiometric character of the image frequently makes it easier to interpret. The distant sensing improvement that is of most interest typically involves edge detection, smoothening, and sharpening.

3.5.1 Image segmentation techniques

Separating an image into homogeneous pixels' sections based on some specific criterion is referred to as image segmentation. This process does not only detect the edge of the object through finding transition on images brightness but also split the images background and foreground in a significant manor. Under this technique we have segmentation based on histogram, hybrid, edge and regions. This research purpose to identify and segments the coastline into vulnerable erosion and accretion areas.

3.5.2 Conversion of image to RGB

Gray scale image has the challenge of viewing the land cover features during data training. It is therefore advisable to convert the gray scale image to RGB so that the vegetation cover is enhanced. In RGB data the dark red depicts dense vegetation cover while light red depicts sparse vegetation. To convert image to RGB the layer stacked image is opened on ENVI 5.3 window. It should be noted that during layer stacking the visible and near infrared bands must be stacked i.e. for Landsat 8 bands 4,3 and 2 must be included. To achieve RGB, merging of bands and channel must be done: Band 4 for red channel, band 3 for green channel and band 2 for blue channel. The resulting RGB image gives the analyst an advantage of viewing vegetative covers.

CHAPTER 4. MATERIALS AND METHODOLOGY.

4.1 Acquisition of Images.

Several images encompassing the area and of period interest were collected using two satellite: (Landsat 5, 7 and 8 and Sentinel-2) to meet the goal of this study. Landsat satellite series has on board different versions of sensors namely: Operational Land Imager (OLI), Enhanced Thematic Mapper plus (ETM+) and Thematic Mapper (TM) operating on the VIS, NIR, SWIR and TIR. Its main objective is to provide current, cloud-free photographs while also updating the worldwide satellite photo library. The Landsat 7 ETM+ sensor, in particular, includes 8 spectral bands, in which bands one to seven and band 8 have spectral resolution of 30m and 15m respectively. Even though Landsat is managed by US Geological Survey (USGS), its images are downloaded from NASA's website. Selection of images in this study was based on image area coverage, cloud cover severity, spatial and spectral resolution and time period availability. It should be noted that Landsat has around 16 days' revisit period.

Sentinel-2 is an earth observation mission from Copernicus program which acquire images over water and land at a high spatial resolution (10m to 60m). This satellite being operated by European space agency (ESA) was launched on 23/6/2015 and became operational on 15/10/2015. To accomplish this task, Sentinel-2 images for period 2015 to 2021 were downloaded from earthexplorer.usgs.gov. The images were geometrically resampled and projected using both SNAP and ENVI 5.3 software. Sentinel-2 data has a total of 13 bands; for this research bands 2, 3, 4 and 8 each having a spatial resolution on 10m were Layer stacked before being classified. The purpose of layer stacking the bands was to view image as a color composite; this is not possible with single bands. Once this was done identification and extraction of endmember to perform class training for supervised classification was possible. Sentinel has a temporal resolution of 2 to 5 days in mid latitudes and 10 days in equator. Table 1 shows acquisition dates of satellite data used.

Table 1: Details of satellite data used their acquisition dates and resolution

Satellite and sensor	Date of acquisition	Path/Raw	Bands used	Spatial resolution
Landsat TM	1990-06-19	166/062	Visible & NIR	30m
Landsat TM	1994-10-12	166/062	Visible & NIR	30m
Landsat ETM+	2000-04-27	166/062	Visible & NIR	30m
Landsat ETM+	2009-09-18	166/062	Visible & NIR	30m
Landsat OLI	2014-03-25	166/062	Visible & NIR	30m
Landsat OLI	2016-12-27	166/062	Visible & NIR	30m
Landsat OLI	2018-04-05	166/062	Visible & NIR	30m
Landsat OLI	2020-04-26	166/062	Visible & NIR	30m
Landsat OLI	2021-03-01	166/062	Visible & NIR	30m
Sentinel-2	2015-11-23	N/A	Visible & NIR	10m
Sentinel-2	2016-03-02	N/A	Visible & NIR	10m
Sentinel-2	2017-10-03	N/A	Visible & NIR	10m
Sentinel-2	2018-04-16	N/A	Visible & NIR	10m
Sentinel-2	2019-04-01	N/A	Visible & NIR	10m
Sentinel-2	2021-02-06	N/A	Visible & NIR	10m
Sentinel-2	2021-03-16	N/A	Visible & NIR	10m

4.2 Image pre-processing

The radiometric and geometric aberrations is a norm to most downloaded satellite data; hence correction is necessary. Factors leading to radiometric correction include; sensor noise, atmospheric correction, radiometric correction, viewing geometry and scene illumination. The stated factors differ from one sensor to another due to environmental condition at the time of data capturing. It should however be noted that, for effective data comparison calibration to reflectance or radiance is necessary as a pre-processing procedure. The purpose of pre-processing is to enhance certain image features necessary for later processing or reduce undesired distortion in the image data. In this study, a few pre-processing techniques are discussed.

4.2.1 Atmospheric correction

Many satellite data such as those from MODIS come handy with atmospheric correction already performed. However, some sensors like Landsat TM/ETM+ lack this advantage; necessitating atmospheric correction. Gaseous absorption, aerosol scattering and Rayleigh scattering in the VIS channels (480nm, 560nm, and 660nm) and NIR channels (830nm) are all taken into account during correction (H. Quaidran,1998).

To achieve radiometric calibration a MLT-Multispectral Landsat image was loaded on ENVI 5.3 via its toolbar. From the resulting file selection dialog box this image was highlighted and converted to reflectance. FLAASH demands that input data to be floating-point values, for this purpose a digit one was entered on single scale factor field.

4.2.2 Layer stacking

It refers to a procedure of merging numerous bands/images into single image. This process is possible if size of images and spatial resolution of the bands are resampled to a target resolution. It should however be noted that the resulting layer stacked image will be voluminous and as a consequence both overall processing and time for analysis are prolonged. Secondly, it is not mandatory that all the bands must be layer stacked but only the specific ones needed by the analyst. This depends on the objective of the study. In this study we layer stack the VIS and UV bands This layer stacking assist in observation of landcover features as a colour composite.

4.2.3 Reprojection

In order to make downloaded photos consistent with global reference systems, distortion is removed through the process of re-projection. The images used in this study were not only reprojected to the World Geodetic System (WGS) 84 Datum and zone 37S of the Universal Transversal Mercator (UTM), but also resampled using the closest neighbor method. The integrity of each spectral image pixel is preserved by this method.

4.2.4 Cloud removal

Cloud cover can compromise the quality of a classified image thus their removed in mandatory. The identification of cloud covers is achieved by transforming the values of TIR DN to temperature brightness (K) values. The concept underlying this process is that the darker parts in TIR band tend to register lower temperature (K) values than normal in comparison to cloud free TIR band. This advantage of thermal variation enables the analyst set temperature (K) threshold to aid in identification and removal of cloud. In this study a threshold of 240 K was set on Landsat 8 data; below which was classified as dark part. It was then possible to remove the dark part by temperature threshold value. The ENVI 5.3 offers a platform to accomplish this task.

4.3 Image processing

The interpretation of remotely sensed images with aid of a computer is referred to as image classification. Identification of spectral signatures of various land cover types forms the basis of classification. Image processing entails spectral signature extraction, data training and classification and its success depends on availability of distinct spectral signature of different endmembers on the target image and the ability to differentiate these signatures from other spectral response patterns present in the image.

The two main methods for classifying images are supervised and unsupervised. They have different approaches in terms of classification. Supervised classification demands for identification of pixels of known land cover types by the user before all pixels in the scene are regrouped into one of these groups by the computer algorithm. Unsupervised classification, on the other hand, uses a computer technique to locate distinct clusters of points in the data space, which are subsequently interpreted by the user as various classes.

4.3.1 Extraction of signatures (endmember file)

Using the k-means clustering technique (Unsupervised classification) image covering the region of interest was classified. This was done purposely to provide analyst with advantage of visualizing the image in order to determine possible landcover types. Ground control points from google earth assisted in features identification.

4.3.2 Data training

For each land cover class, the locations that served as training grounds were identified. The two different temporal sets of scenes of most recent images were loaded in Google Earth after being registered to geographic locations using a GPS device. To achieve this, a second order polynomial was computed to transform the line and column locations of selected pixels across the image to their latitude and longitude locations; which was determined from the map and ground control point (G.C.Ps) data. The exact locations of pins at the area's center were determined using the Google Earth software.

4.3.4 Image classification

Supervised classification approach make two assumptions while computing classification: Trajectory of cover types attributes can be categorized into meaningful discrete features; these features can be mapped from satellite data (Ahmad and Quegan, 2012). Background information about the research area, either from outside sources or through fieldwork, is necessary for supervised classification. Be it maximum likelihood (ML) algorithm or Spectral angular mappers (SAM) data training is a mandatory procedure.

Data retrieved from ROIs (“seeds”) are the determinant of good classification and mapping of ecological systems such as; morphodynamics, forests and wetlands. Regions with various endmembers tend to have ROIs with complex heterogeneous system (Berhane et al., 2019). In this study both ML and SAM algorithms were used to classify the study area. The training data (ROIs) and spectra collected in spectral library were retrieved and both used to classify the study area. The landcover types include; mangrove, bare land, water, shrubs and settlement. The classified results from the two techniques were compared with more advantage attributed to ML algorithm. The flow chart for the aforementioned processes is shown in Figure 8 below.

Flow chart

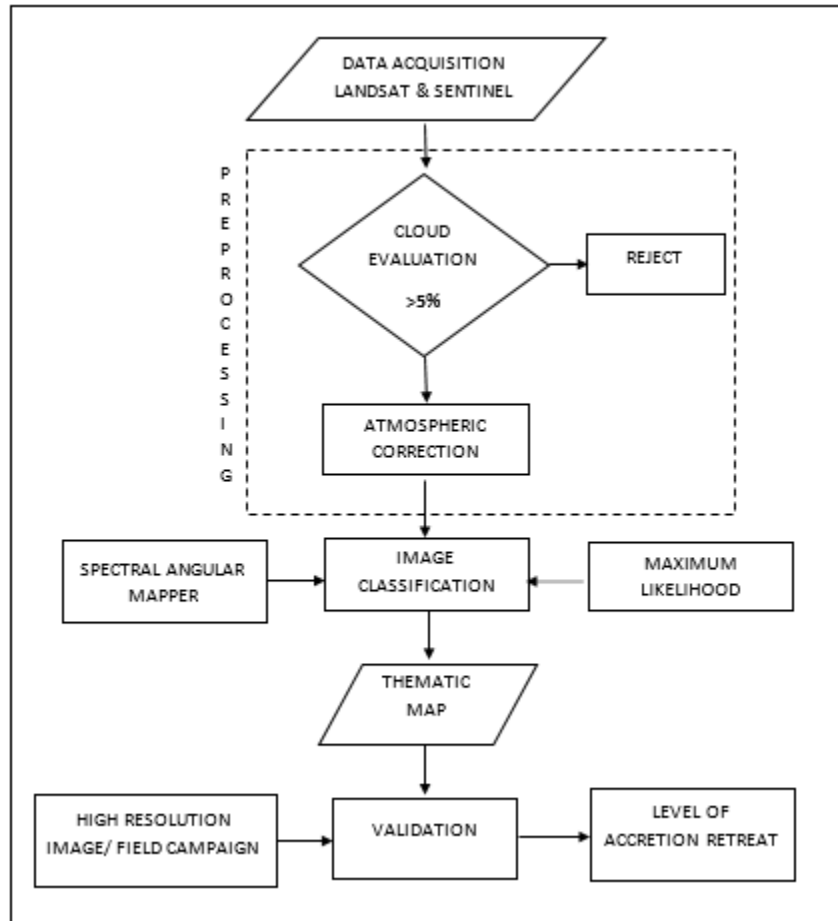


Figure 8: A flow chart showing image pre-processing, processing and post processing

4.4 The concept of Accuracy assessment

Be it supervised or unsupervised, evaluating the accuracy of the final classified image produced is a crucial stage in the classification process. Field campaign was conducted in the study area by navigated to the location using GCPs loaded in our GPS gadget. Using GPS machine, the location for each endmember was taken by standing at the center of approximately 30x30m area of each endmember. Congalton recommends that in order to evaluate the accuracy of any image classification, at least 50 sample points for each land-use and land-cover category in the error matrix be gathered (Macleod and Congalton, 1998). The sample of points picked were loaded on ENVI 5.3 platform and used to reclassify the area based on new findings. By comparing initially and newly classified, confusion matrix was generated. Equation 5 shows accuracy assessment formula

$$\text{Overall accuracy(OA)} = \frac{N_{AA} + N_{BB} + N_{CC}}{N} \times 100\% \quad (5)$$

Where, N is the total number of points and N_{AA} , N_{BB} , ..., N_{ZZ} are endmembers correctly classified (sum of elements in main diagonal of the confusion matrix).

CHAPTER 5. RESULTS AND DISCUSSION

5.1 Classified Landsat Data

This chapter discusses the results of applying maximum likelihood techniques, as outlined in Chapter 4, to construct thematic maps of evolving coastline along the Mto Tamamba area. Temporal coastal change (areas of erosion and accretion) has been represented by comparing multi-temporal and multi-scale remote sensing imagery with aid of ENVI 5.3 and ArcGIS 10.2 software. Figure 9 depicts a progressive change in land scape an effect of gradual deposit of sediments along the Mto Tamamba area from 1990 to 2021 for Landsat data. The dark green depicts mangrove vegetation, light green for shrubs while the brown depicts bare land. Bare land in this context refers to rocks and all kind of soils. The chronological advancement of endmember bare land can be seen clearly in this figure. The findings also show that majority of the coastline along the Mto Tamamba has been prograding. This could be owing to the lack of development along this length of shoreline and the availability of dense mangrove forest. The presence of young mangrove plants in this location may be a contributing factor in the accumulation of sediments. Another major contributor to this threat is the regular entry of ocean waters into the land (a common feature of coastal beaches), to which Kenya is not immune. On a daily basis, water dynamics in the form of waves sweep the ocean bed and erode the sediments onshore. When water returns to the ocean, it does so gradually, leaving behind silt that contributes to accretion. The sediments left behind are rich in dead microorganisms, which promote mangrove germination. Most settlements in this area are temporary structures which are built by fishermen who migrate depending on availability of fish. Due to scanty population in this area, mangroves have been able to establish themselves well providing strong line of defense thereby avoiding land loss.

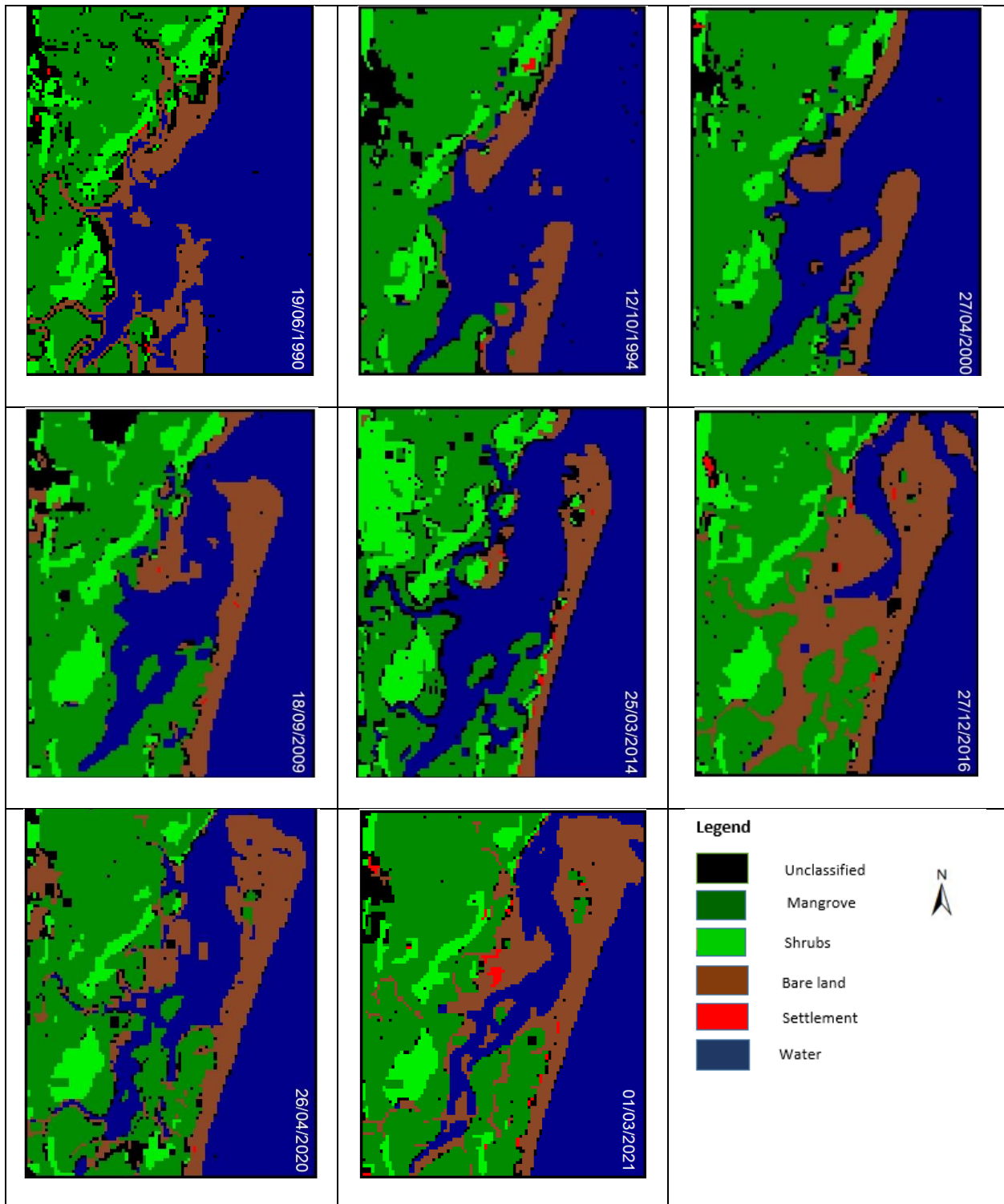


Figure 9: Classified images for mto Tamamba area trend change from 1990 to 2021

5.2 Thematic change between 1990 and 2021

Figure 10 depicts thematic changes along the shoreline of Mto Tamamba delta from 1990 to 2021. The results show that there was erosion and prograding throughout that period in the study area. The findings revealed an overall increase in bare land, indicating either downstream push of top alluvial soil or Sea bed erosion over time. The red part of the image depicts an increase in bare land inside water surrounding Mto Tamamba. The dark green emphasizes places that have transitioned from bare land to mangrove throughout the years, while the light green highlights areas that have transitioned from bare land to shrubs over the 31-year period. The grey shows unchanged areas. A ground truthing operation was done to confirm the desktop application. The general impact of this menace is that the coastline is shifting towards the ocean.

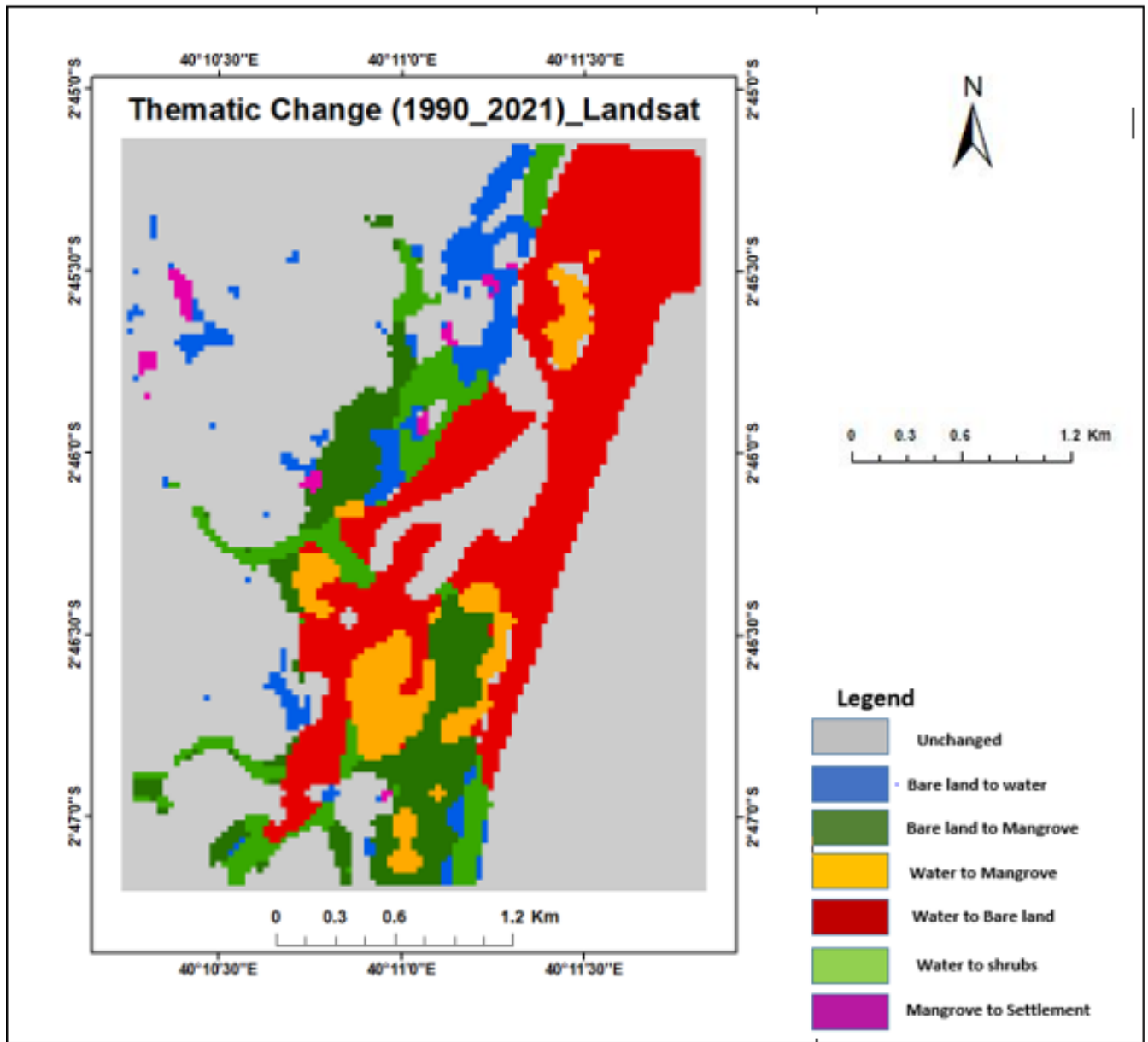


Figure 10 : Image showing thematic change of land cover between 1990 and 2021

5.3 Change detection statistics for Landsat between 1990 and 2021

ENVI 5.3 software was used to generate the change statistics over the two periods (1990-2021). The change statistics was calculated to describe the movement of the coastline over time to its current position. There are a range of statistical change measures derived from ENVI 5.3 based on the pixels counts of the classified image over time. In Landsat data one pixel is approximately equal to 900 m². Table 2 compares statistical values of endmembers for two sets of image namely initial (1990) and final (2021). Negative value implies a decrease while positive implies and an increase. From the table it is observed that the endmember water decreases by 1923 pixels over the 31-year period. Over these years, the area covered by mangrove expanded by 1562 pixels counts. Both bare land and settlement increased by 1074 and 68 pixel counts respectively while shrubs decreased by 158 pixel counts. The increase in mangroves in the study region can be attributed to the increase in barren land since the fertile top alluvial soil is conducive for the establishment of vegetation. The slight increase in settlement is due to the economic activities of the people who live in the region; this area is primarily occupied by fishermen who relocate regularly in quest of good fishing ground.

Table 2: Landsat thematic change detection statistics.

		Area per Pixel count						
		Initial Stage-1990						
		Unclassified	Water	Mangrove	Shrubs	Bare land	Settlements	Total Raw
Final Stage-2021	Unclassified	603	65	20	99	60	3	850
	Water	163	3235	35	126	224	0	3783
	Mangrove	483	552	2868	127	584	0	4614
	Shrubs	94	0	108	535	23	6	766
	Bare land	116	1835	21	23	486	1	2482
	Settlements	14	19	0	14	31	0	78
	Class total	1473	5706	3052	924	1408	10	
	Class changes	870	2471	184	389	922	10	
Image difference	-623	-1923	1562	-158	1074	68		

Figure 11 shows graphical presentation of distribution of endmembers in the study area between 1990 and 2021. The graph depicts a decrease in area covered by both endmembers water and shrubs over the study period whereas area occupied by mangrove and bare land have generally increased. This is in line with information obtained in table 2.

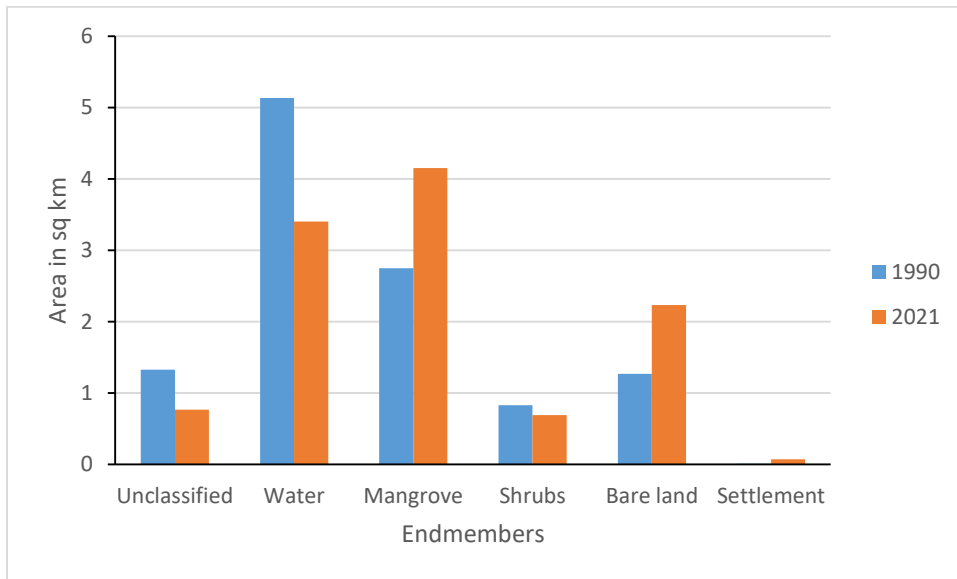


Figure 11 : Landsat change detection statistics (1990-2021)

5.4 Linear regression plots showing area in square Km covered by each endmember for Landsat data.

Figure 12 shows scatter plots for each endmember in the Mto Tamamba area as presented by excel software. The endmember bare land exhibit positive trend in scatter distribution with $R^2 = 0.5914$ while the endmember water exhibit negative trend with $R^2 = 0.7403$. The R^2 for bare land is quite low due to the challenge of getting consistent cloud free Landsat images over the period of study. Mangrove forests have a positive linear regression and the same applies to settlement. The negative line trend for endmember water may be attributed to reduction of pixel covered by water body. It should be noted that the endmember settlement depicts a slight positive trend; this may be due lack of permanent settlement in this area a pattern exhibited by fishermen.

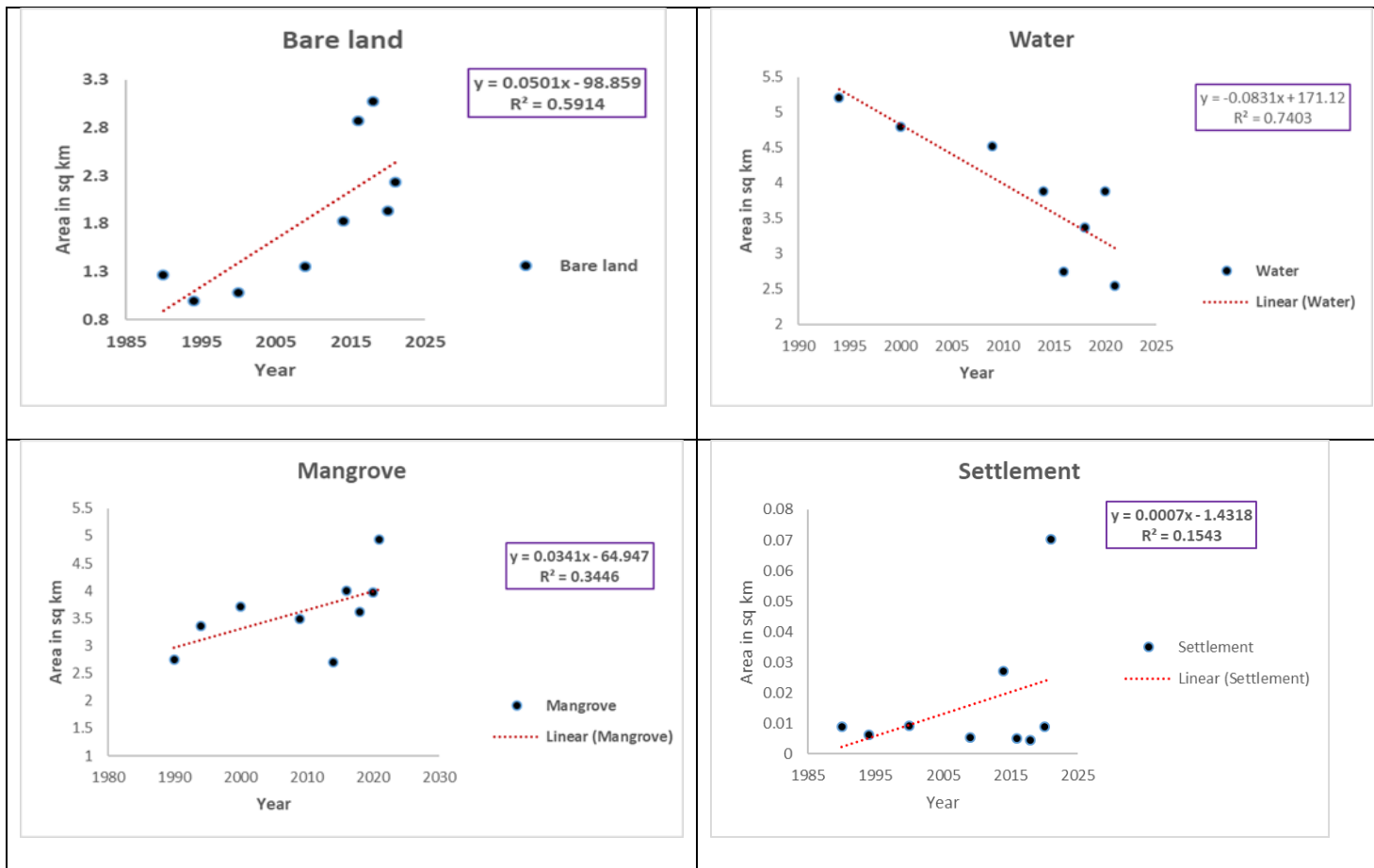


Figure 12: Linear regression graphs from Landsat data.

5.5 Correlation plots for Land cover types.

Figure 13 below exhibit correlation plots for pairs of endmembers. This was purposely done to investigate how any given two endmembers relate over time. In this figure it is observed that the endmembers water and bare land exhibit a correlation, with $R^2= 0.5138$. Endmembers bare land and vegetation, on the other hand have a positive correlation with $R^2=0.468$. It is concluded from this correlation plot that an increase in bare land towards the ocean results in a decrease in the area of pixels initially occupied by water. This supports the observation made in Figure 10 by thematic change. The fact that land is seen prograding towards the ocean is an indication that sediment is piling in this region. The vegetation and bare land have a favorable link because eroded soil contains fertile alluvial deposit, which encourages the growth of sparse and dense vegetation such as mangrove forest. It should be noted that in this region, water is advancing into the land on a daily basis between noon and 6 p.m. This daily water advancement facilitates dispersion of mangrove seedling into the land. This water gradually returns back in the Ocean from mid night leaving sediments behind. This process eventually leads to evolution of the coastline.

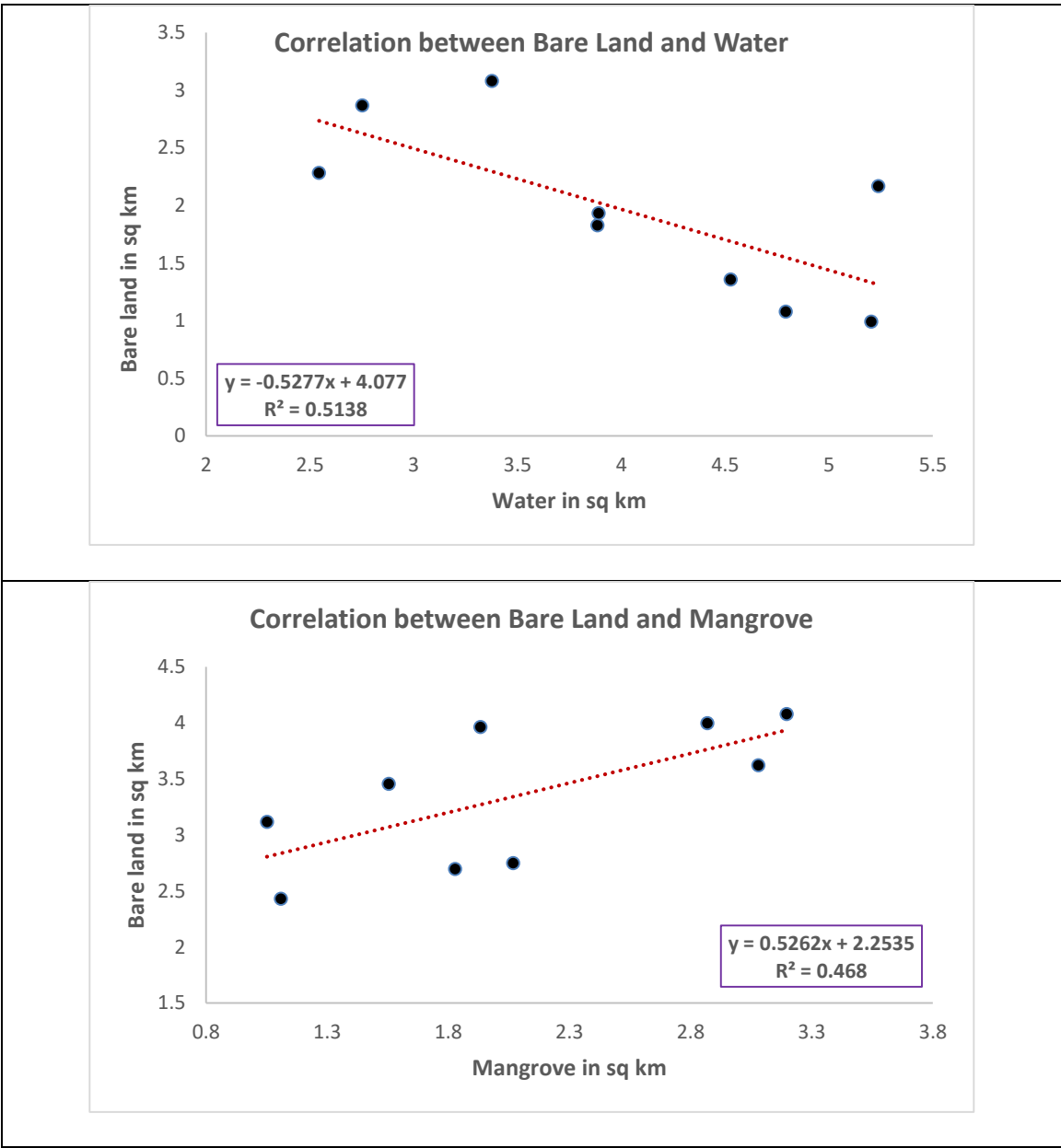


Figure 13: Correlation graphs comparing relation of endmembers in Landsat data.

5.6 Classified Sentinel-2 Data

To assess the extent of erosion or accretion in the study area, the maximum likelihood classification method was also used to classify the Sentinel 2 images. This was purposely done to establish whether the temporal distribution trends depicted by Landsat cover types conforms with that of Sentinel-2 data. Just like Landsat, Sentinel-2 data is freely accessed. It should however be noted that its late launch (27th June 2015) makes it unpopular for studies that require long-term monitoring. Nevertheless, with temporal resolution of 2 to 5 days it was possible to get more cloud free images with Sentinel-2 as compared to Landsat whose repeated coverage is about 16 days. In this study images between 2015 and 2021 were used and the same landcover types as in Landsat images maintained. The selected images showing the spatial changes of landscape between 2015 to 2021 are displayed in Figure 14. Dark blue portions represent water pixels, dark green areas represent mangroves, light green pixels emphasize shrubs, and red pixels' highlight habitation in the research area. Brown areas correspond to barren land pixels. This finding establishes that the class bare land has generally increased over time while that of water has decreased. This is consistent with results obtained from Landsat data.

Figure 14 shows that the study area was experiencing prograding over the years 2015-2021. This accretion can be attributed to the presence of mangrove forest in this area that provide a strong line of defense preventing the carrying away of sediments into the Ocean. Eventually the sand eroded from the sea bed piled along the shore line leading to evolution. Another main reason for prograding is the presence of salt factory around this region which pumps water on daily basis for the purpose of desalination. This leads to decrease in sea level exposing more sediments hence necessitating the piling of sand.

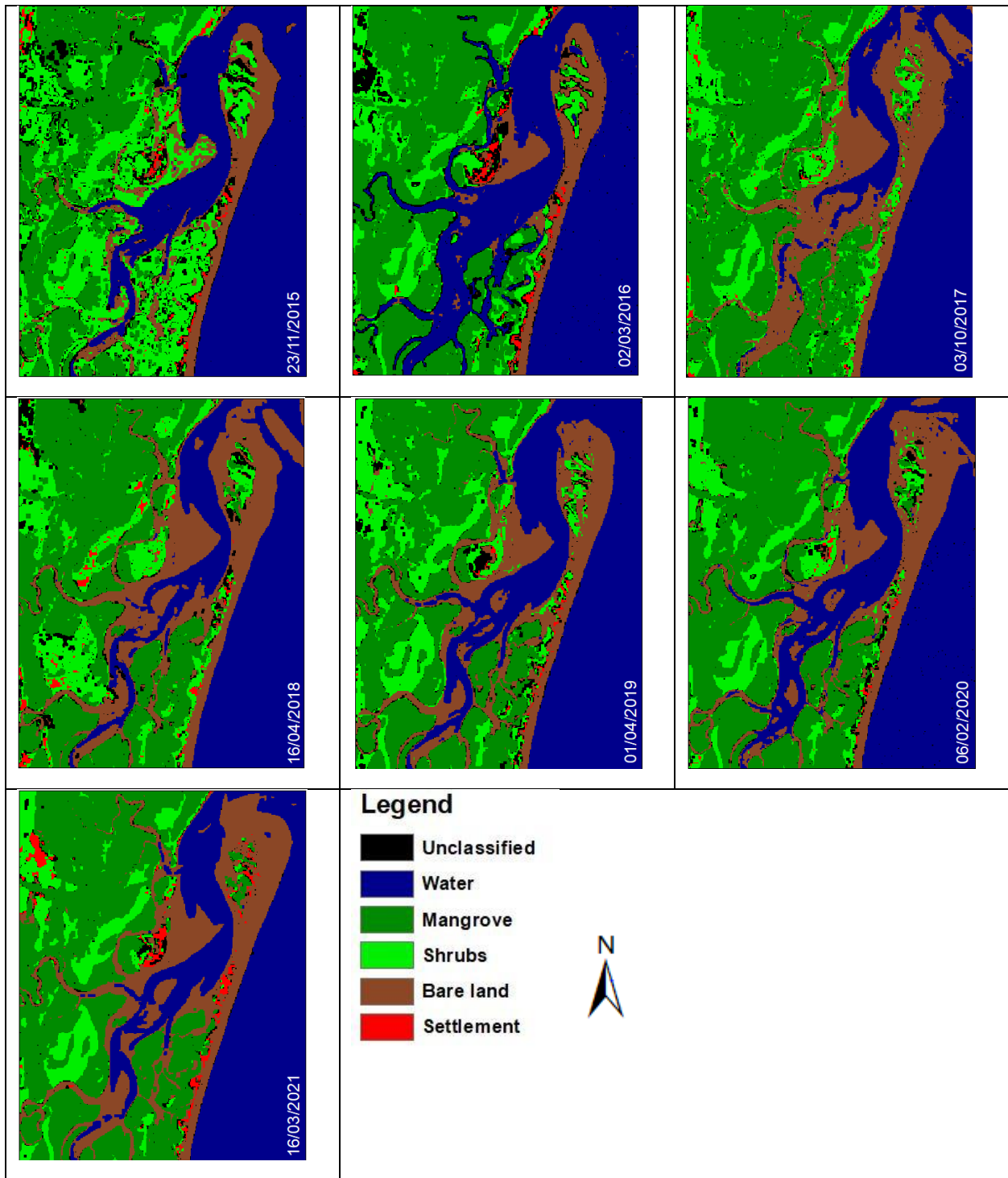


Figure 14: Classified Sentinel-2 image showing trend of land cover change from 2015-2021

5.7 Thematic change detection for Sentinel 2 data

Using ENVI 5.3 software, thematic change detection technique was applied on 2015 and 2021 classified images. Figure 15 shows the results of the thematic change. The red part of the image depicts an increase in bare land inside water surrounding Mto Tamamba area. The dark green emphasizes places that have transitioned from bare land to mangrove throughout the years, while the light green highlights areas that have transitioned from bare land to shrubs over the 6-year period. It is observed that the class bare land (in red) has sifted inside the Ocean. The period of study was shorter due to time of Launch of Sentinel-2 satellite (27th June 2015). It should be noted that this satellite became operational on 15th October 2015.

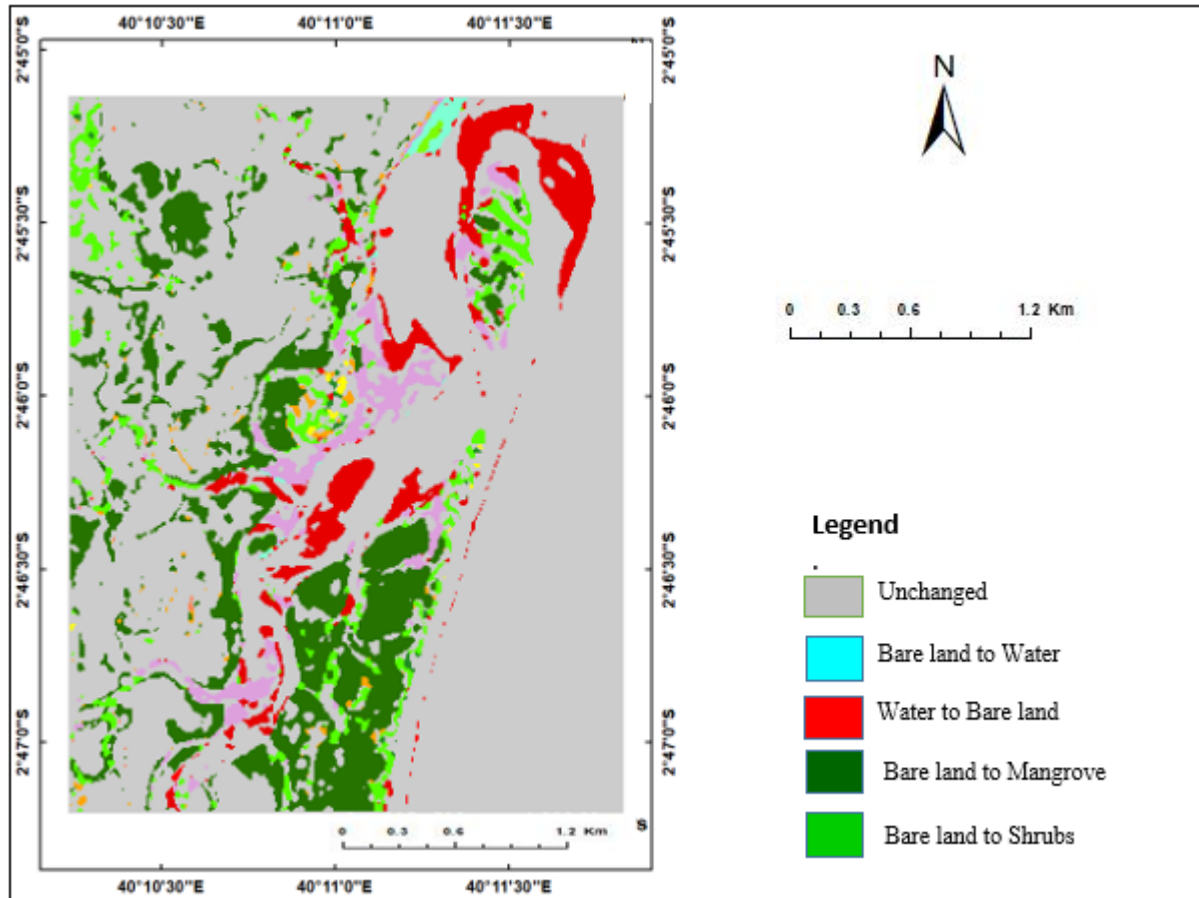


Figure 15: Image showing thematic change of Sentinel-2 image between 2015 and 2021

5.8 Change detection statistics for Sentinel-2 between 2015-2021

Using ENVI 5.3 change detection was done for 2015 and 2021 classified images. The findings in Table 3 revealed an overall increase in number of pixels occupied by bare land by 9704 (0.9704 km²) an indication that top alluvial soil has been pushed downstream over the six years under study. However, the pixels' coverage for water decreased by 4508 (0.4508 km²). It should be noted that based on spatial resolution of Sentinel-2 the area of each pixel is 100m². These data concur with results obtained from Landsat data. Ground truthing operation was done in this study area confirmed the existence of prograding land.

Table 3: Change detection statistics for Sentinel-2 (2015-2021)

		Area per Pixel count						
		Initial Stage-2015						
		Unclassified	Water	Mangrove	Shrubs	Bare land	Settlements	Total Raw
Final Stage-2021	Unclassified	2051	752	1167	341	488	75	4874
	Water	279	32409	142	276	738	101	33945
	Mangrove	2306	43	30878	8043	451	0	41721
	Shrubs	844	0	1739	6937	20	344	9884
	Bare land	1010	5249	5704	87	8458	40	20548
	Settlements	601	0	138	256	689	416	2100
	Class total	7091	38453	39768	15940	10844	976	
	Class changes	5040	6044	8890	9003	2386	560	
Image difference	-2217	-4508	1953	-6056	9704	1124		

Figure 16 shows bar graphs presentation of area covered in square kilometer of endmembers in the study area for years 2015 and 2021 as extracted from classified Sentinel-2 data. The graph depicts a decrease in area covered by both endmembers water and shrubs over the study period whereas areas occupied by mangrove and bare land have generally increased. This is consistency with information obtained in table 3 under thematic change. The data also concur with information obtained in Figure 11 under Landsat data. The only difference is the smaller area covered by each landcover types which is due to shorter period of study (6 years).

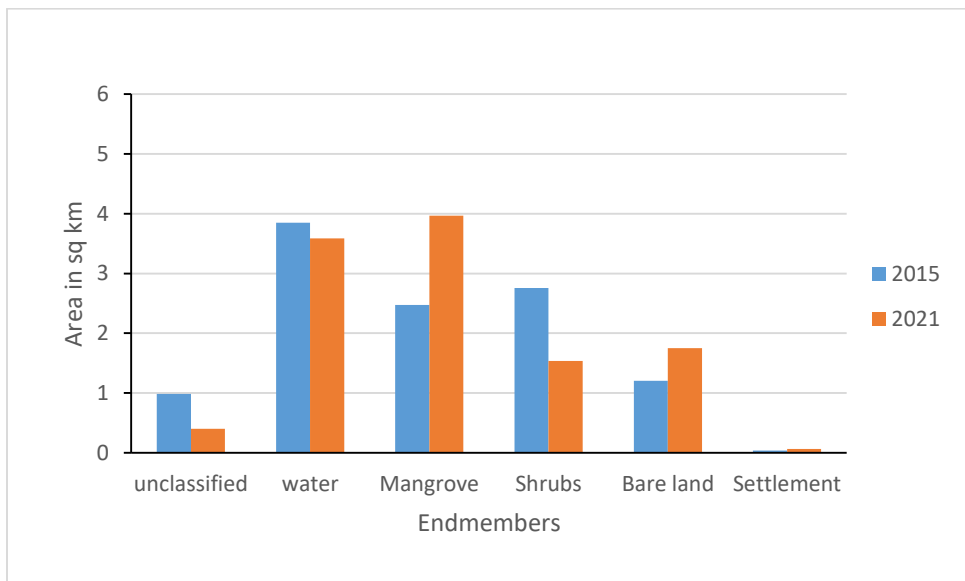


Figure 16: Sentinel change detection statistics (2015-2021)

5.9 Linear regression plots showing area in square Km covered by each endmember for Sentinel data

The class statistics obtained from endmembers in the study area were plotted and their results conveyed in figure 17. The scatter plots for endmember bare land gave a positive gradient with $R^2 = 0.2387$ while that obtained from water depicts a negative trend with $R^2 = 0.0681$. The endmember mangrove depicts a positive trend with $R^2 = 0.3846$ which might be due high nutrient content in eroded silt which makes it conducive for vegetation to thrive. The low values of R^2 for these endmembers may be attributed to shorter period of study (6 years) as well as inability to get many cloud free images using Sentinel-2 data. Change in coastal morphology is a long-term phenomenon that require many years' data for effective results. Nevertheless, the trend is at par with Landsat data.

Figure 18 shows correlation graphs for bare land and water having a $R^2 = 0.7857$. It can be deduced from this correlation plots that an increase in bare land led to decrease in pixel occupied by water body. This is an indication that bare land is eating up pixels previously occupied by water in the study area an evidence of sediments piling in water area hence accretion. On the other hand, the correlation plot between bare land and mangrove is a positive slope with $R^2 = 0.4305$. This implies that the eroded top fertile alluvial soil has provided conducive environment for the growth of vegetation and in this case the mangrove vegetation. The low value of R^2 (0.4305) may be attributed to hot climatic conditions at the coast as well as logging of trees and fetching of firewood which is common in this area.

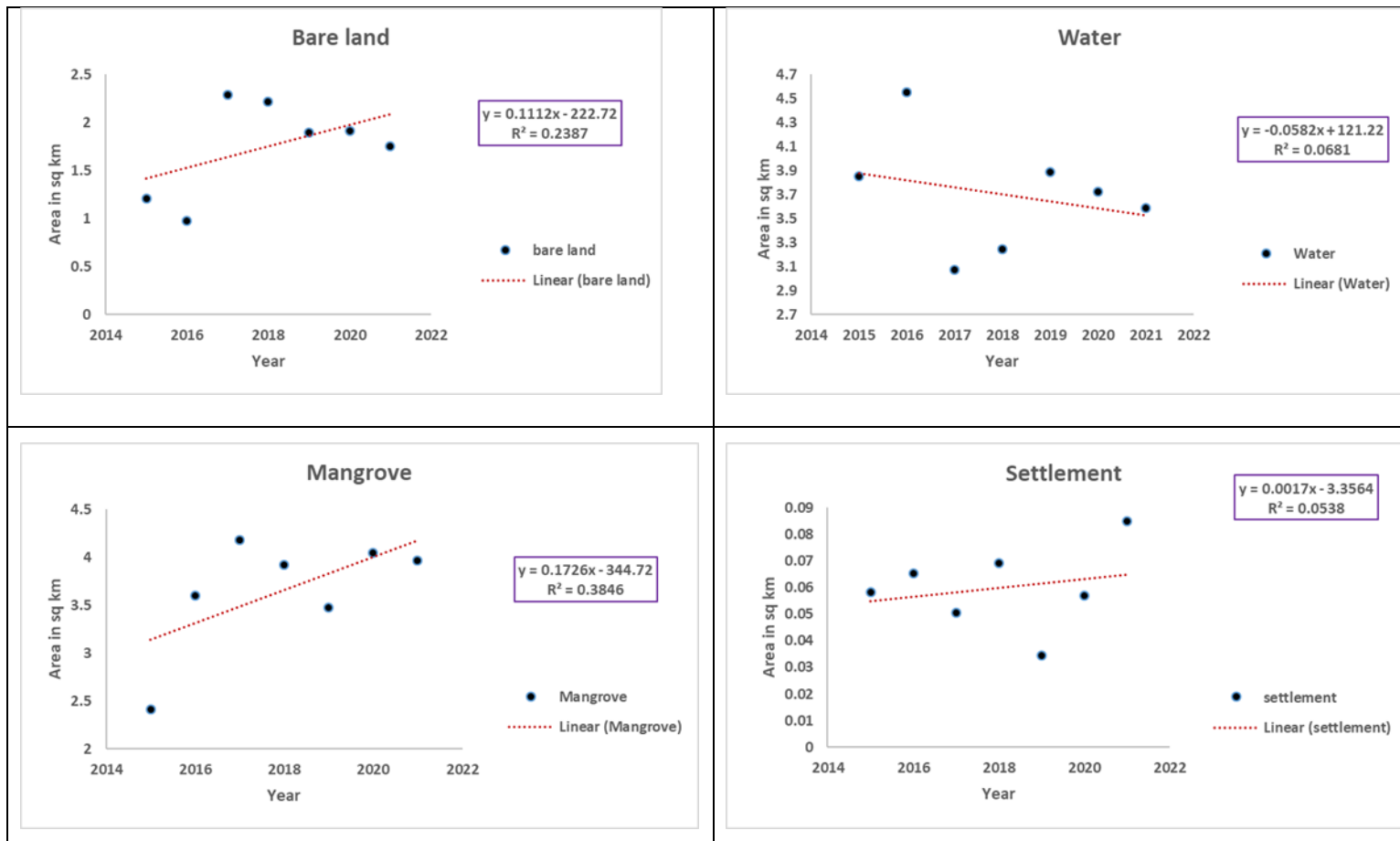


Figure 17: Linear regression plots showing trends for endmember 2015-2021 from Sentinel data

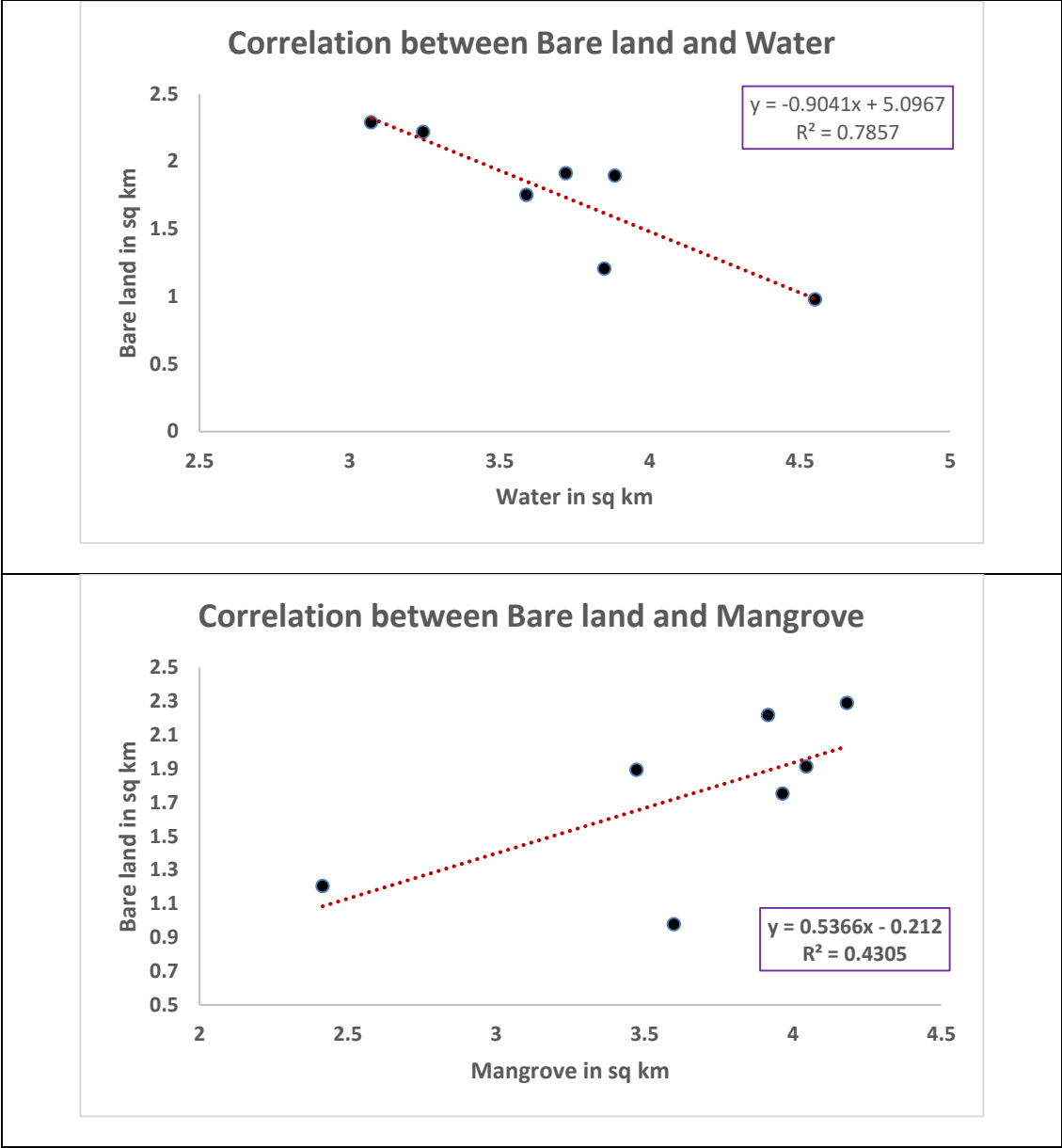


Figure 18: Correlation plots for endmembers (Sentinel-2 data)

5.10 Accuracy assessment report for classified images

The accuracy of a classification is assessed by contrasting the classified data with a reference data set that precisely depicts the real land cover. Some of the sources of reference data are maps created from interpreted aerial pictures, high-resolution satellite images, and actual GPS locations. The accuracy rating compares and takes into account the discrepancy between the categorization and the reference data. The investigation employed supervised classification on both Landsat and Sentinel-2 images. The percentage of the entire area that is accurately mapped is what is meant by "overall accuracy." This suggests that the likelihood of a random point being correctly identified in the target area (reference).

Another gauge of general accuracy with a maximum scale is the kappa coefficient (100 percent). The relative decrease in error produced by a classification procedure as opposed to the error of a purely random classification is expressed by kappa statistics (reference). During the field trip, Fundisha sub-location (study area) in Marereni location was visited and a total of 50 location points based on endmembers were picked at random using GPS machine and recorded for purpose of validation. This was realized by standing at the center of approximately 30 by 30 m area covered by a specific endmember and picking the point using GPS machine. Table 4 below shows the GPS location of various land cover types collected from the study area during field campaign between 1st to 5th Oct 2021. These in situ-measurements were used to compute confusion matrix for both Landsat and Sentinel-2 images.

Table 4: In situ- measurements collected from field campaign

Satellite Overpass		Field Campaign			Landcover
Path/Raw	Date	Latitude	Longitude	Date	
166/062	01.10.2021	-2.7533	40.1829	02.10.2021	Mangrove
166/062	01.10.2021	-2.7585	40.1805	02.10.2021	Mangrove
166/062	01.10.2021	-2.7639	40.1821	02.10.2021	Mangrove

166/062	01.10.2021	-2.7533	40.1751	02.10.2021	Shrubs
166/062	01.10.2021	-2.7773	40.1756	02.10.2021	Shrubs
166/062	01.10.2021	-2.7572	40.1841	02.10.2021	Bare land
166/062	01.10.2021	-2.7572	40.1719	02.10.2021	Bare land
166/062	01.10.2021	-2.7588	40.1712	02.10.2021	Settlement
166/062	01.10.2021	-2.7545	40.1844	02.10.2021	Settlement
166/062	01.10.2021	-2.7507	40.1750	02.10.2021	Mangrove
166/062	01.10.2021	-2.7634	40.1728	02.10.2021	Shrubs
166/062	01.10.2021	-2.7543	40.1847	02.10.2021	Shrubs
166/062	01.10.2021	-2.7651	40.1933	02.10.2021	Bare land
166/062	01.10.2021	-2.7667	40.1832	02.10.2021	Settlement
166/062	01.10.2021	-2.7607	40.1861	02.10.2021	Water
166/062	01.10.2021	-2.7584	40.1878	02.10.2021	Water
166/062	01.10.2021	-2.7568	40.1753	02.10.2021	Mangrove
166/062	01.10.2021	-2.7681	40.1914	02.10.2021	Bare land
166/062	01.10.2021	-2.7619	40.1912	02.10.2021	Settlement
166/062	01.10.2021	-2.7668	40.1893	02.10.2021	Water
166/062	01.10.2021	-2.7674	40.1913	03.10.2021	Water
166/062	01.10.2021	-2.7700	40.1858	03.10.2021	Water
166/062	01.10.2021	-2.7623	40.1743	03.10.2021	Mangrove
166/062	01.10.2021	-2.7615	40.1907	03.10.2021	Mangrove
166/062	01.10.2021	-2.7683	40.1893	03.10.2021	Bare land
166/062	01.10.2021	-2.7735	40.1904	03.10.2021	Bare land
166/062	01.10.2021	-2..7708	40.1840	03.10.2021	Settlement

166/062	01.10.2021	-2.7605	40.1815	03.10.2021	Shrubs
166/062	01.10.2021	-2.7609	40.1844	03.10.2021	Shrubs
166/062	01.10.2021	-2.7591	40.1866	03.10.2021	Water
166/062	01.10.2021	-2.7586	40.1731	03.10.2021	Mangrove
166/062	01.10.2021	-2.7602	40.1824	03.10.2021	Shrubs
166/062	01.10.2021	-2.7853	40.1862	03.10.2021	Bare land
166/062	01.10.2021	-2.7816	40.1869	03.10.2021	Bare land
166/062	01.10.2021	-2.7708	40.1781	03.10.2021	Bare land
166/062	01.10.2021	-2.7856	40.1712	03.10.2021	Settlement
166/062	01.10.2021	-2.7623	40.1723	03.10.2021	Settlement
166/062	01.10.2021	-2.7846	40.1866	03.10.2021	Water
166/062	01.10.2021	-2.7835	40.1776	03.10.2021	Water
166/062	01.10.2021	-2.7843	40.1729	03.10.2021	Shrubs
166/062	01.10.2021	-2.7797	40.1723	03.10.2021	Shrubs
166/062	01.10.2021	-2.7692	40.1899	04.10.2021	Mangrove
166/062	01.10.2021	-2.7571	40.1712	04.10.2021	Settlement
166/062	01.10.2021	-2.7607	40.1921	04.10.2021	Settlement
166/062	01.10.2021	-2.7656	40.1832	04.10.2021	Settlement
166/062	01.10.2021	-2.7818	40.1887	04.10.2021	Water
166/062	01.10.2021	-2.7621	40.1875	04.10.2021	Water
166/062	01.10.2021	-2.7697	40.1896	04.10.2021	Settlement
166/062	01.10.2021	-2.7655	40.1753	04.10.2021	Mangrove
166/062	01.10.2021	-2.7852	40.0194	04.10.2021	Shrubs

5.10.1 Satellite overpass

It should however be noted that, for effective accuracy assessment, satellite overpass time should concur with time of field campaign. This ensures that the position of actual land cover type picked during insitu-measurements are at par with those taken by sensor. Landsat satellite overpass on study area was on 1/10/2021 just one day before our data was picked. Satellite overpass dates for Landsat data can be accessed through U.S.G.S global viewer (<https://glovis.usgs.gov/>). The main reason for making field campaign as close as possible with satellite overpass is to minimize land surface changes that may arise due to change in position of some land cover types during the sensor pick.

5.10.2 Validation results

Using ENVI 5.3 the collected GPS points in table 4 were used to generate confusion matrix with Landsat data giving an overall accuracy of 84% and kappa coefficient of 0.7989. On the other hand, Sentinel-2 data gave an overall accuracy and Kappa coefficient of 88% and 0.8496 respectively. It should be noted that Sentinel-2 gave a higher level of accuracy not only due to advantage of repeated coverage of 2 to 5 days but also its high spatial resolution of 10m. It was also possible to get more images with minimal cloud cover with Sentinel-2 than with Landsat. Tables 5, 6, 7 and 8 show the validation results from

Table 5: Confusion matrix for Landsat data

Class	Water_1	Mangrove_1	Shrubs_1	Bare land_1	Settlement_1	User Total
Water	9	0	0	2	0	11
Mangrove	1	8	0	0	0	9
Shrubs	0	2	10	0	0	12
Bare land	1	0	0	9	2	12
Settlement	0	0	0	0	6	6
Producer Total	11	10	10	11	8	50

Overall Accuracy= (42/50) 84.00%

Kappa coefficient = 0.7989

Table 6: Omission and Commission error for Landsat data

	Commission(%)	Omission (%)	Prod.Acc (%)	User.Acc (%)
Water	18.18	18.18	81.82	81.82
Mangrove	11.1	20	80	88.89
shrubs	16.67	0	100	83.33
Bare land	25	18.18	81.82	75
Settlement	0	25	75	100

Table 7: Confusion matrix for Sentinel-2 data

Class	Water_1	Mangrove_1	Shrubs_1	Bare land_1	Settlement_1	User Total
Water	9	0	0	1	0	10
Mangrove	0	10	2	0	0	12
Shrubs	0	1	7	0	0	8
Bare land	1	0	0	10	0	11
Settlement	0	0	1	0	8	9
Producer Total	10	11	10	11	8	50

Overall Accuracy= (44/50) 88.00%

Kappa coefficient = 0.8496

Table 8: Omission and Commission error for Sentinel-2 data

	Commission(%)	Omission (%)	Prod.Acc (%)	User.Acc (%)
Water	10	10	90	90
Mangrove	16.67	9.09	90.91	83.33
shrubs	12.5	30	70	87.5
Bare land	9.09	9.09	90.91	90.91
Settlement	11.11	0	100	88.89

5.11 Resampling of Landsat to 10m resolution

Images from various sensors often have different spatial resolution. To compare such images, resampling either to higher or lower resolution is necessary. This section compares resampled images from Landsat-8 30m with Sentinel-2 10m images with intention of establishing accuracy of classification results from insitu-measurements obtained during field campaign. To achieve this, data from Landsat 8 with a spatial resolution of 30m was resampled to a spatial resolution of 10m using cubic convolution technique. The goal of this procedure was to increase the spatial resolution of Landsat data and classify it to enable comparison between this image and the classified Sentinel 2 image.

5.11.1 Resampling procedure

From basic tools in ENVI 5.3 software layer stacking was selected, on the resulting layer stacking parameter dialogue box a preprocessed Landsat 30m spatial resolution was uploaded. The image was then re-projected to UTM (datum WGS-84). The X and Y pixel size values were changed from 30m to 10 spatial resolutions before selecting resampling technique as cubic convolution. The image resulting from above process was saved awaiting classification. Figure 19 shows a classified resampled Landsat 10m spatial resolution image alongside Sentinel-2 image.

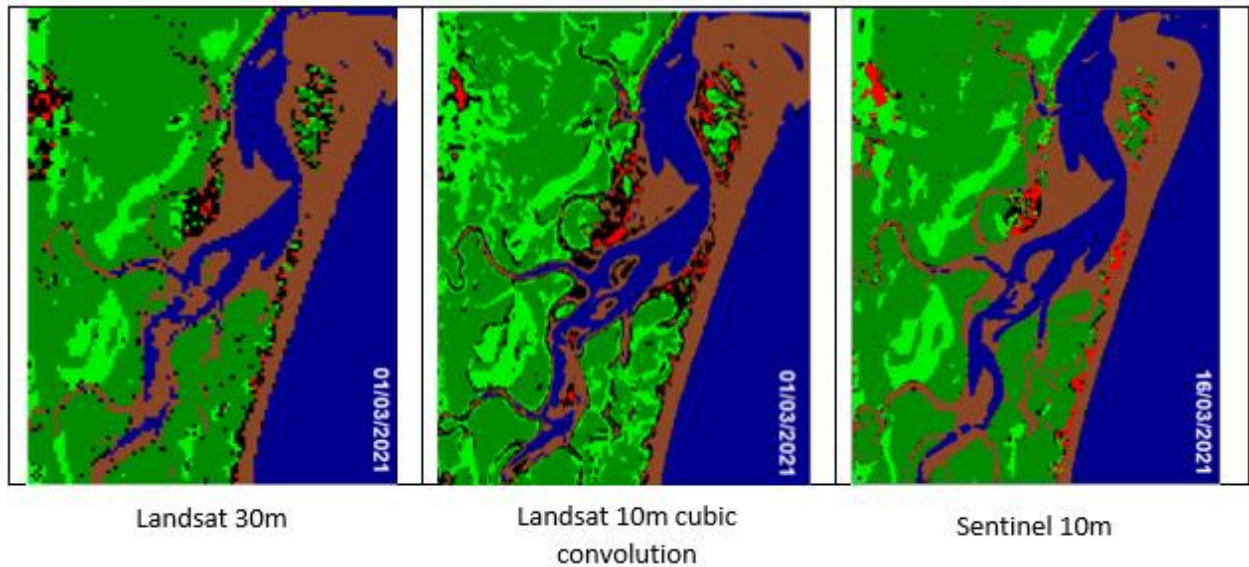


Figure 19: Landsat 30m resampled to 10m resolution using cubic convolution method.

5.11.2 Confusion matrix after resampling

Upon classification of resampled Landsat image, Sentinel-2 image was used as reference data to generate a confusion matrix. To achieve this, data training was done on Sentinel-2 unclassified image using ML technique then 10 correctly classified points of each land cover type were picked at random from sentinel-2 image and used to generate confusion matrix based on classification result of Landsat 8. The result is tabulated in table 9

Table 9: Confusion matrix for Sentinel-2 and Landsat 8 data.

Class	Water_2	Mangrove_2	Shrubs_2	Bare land_2	Settlement_2	User Total
Water	7	0	0	0	0	7
Mangrove	0	9	0	0	0	9
Shrubs	0	1	10	0	0	11
Bare land	3	0	0	10	0	13
Settlement	0	0	0	0	10	10
Producer Total	10	10	10	10	10	50

Overall Accuracy = (46/50) 92.0%

Kappa Coefficient = 0.900

The results show an overall accuracy of 92% an indication that, Sentinel-2 data with a higher spatial resolution can be used to validate Landsat data. It can be seen clearly from this finding that validation via Sentinel-2 data gives a better result as compared to that obtained from in situ-measurements that gave an overall accuracy of 84% and 88% respectively, for Landsat and Sentinel-2 data. Therefore, it is worth noting that, validation of classification results using a higher spatial resolution data can aid in assessing impact of resolution on classification results.

5.12 Discussion

The study of coastline erosion and accretion using remote sensing and GIS techniques has provided realistic information about the state of this section of Kenyan coastline. This study has used both Landsat and Sentinel 2 data on ENVI 5.3 and ArcGIS 10.2 platform to monitor erosion and accretion along this coastline. The fact that the outcome reveals a land prograding North-Eastwards inside the Ocean, suggests that the objective of using thematic change and time-series technique to monitor and map evolution of coastline was successful. Further details reveal that endmembers mangrove, shrubs and some settlements were slowly creeping on the new area; an indication that the process of erosion and accretion has been long to warrant the growth of vegetation and support life of ecosystem. Field campaign confirms the participation of erosion and influence of water dynamics as key contributors of this menace. The change in land-sea interface due to natural and human influence has clearly been depicted in this outcome (Kostiuk and Geography, 2002). Indeed, the participation of erosion and water dynamics has dramatically changed the shape of this part of Kenyan coastline.

The climate at the Kenyan coast is tropical humid therefore the challenge of cloud cover is obvious. This challenge has made many researchers avoid using satellite data. This study provides, to the best of our knowledge the first application of RS and GIS in monitoring Kenyan coastline. In this study, coastline change has been visualized and analyzed consistently through time and space. With extraction of endmember pixel area statistics, time series trend for each endmember was

established. The hypothesis that this coastline evolution might have been triggered by gradual accumulation of sediment from both Indian ocean and Mto Tamamba bed appear to have been confirmed as depicted by both thematic maps (figure 10 and figure 15) and time series trend. The output provides a powerful new insight into pattern and process of coastal morphology by significantly showing coastline change that could not easily be achieved by field survey.

Ground truthing exercise establishes that the main cause of this evolution is among others erosion of Tamamba river bed as well as hydrodynamic effect on the seabed; another contributing factor is daily recession of Indian Ocean water (negative surge) that floods the land carrying along with it dead aqua micro-organisms (MacDonald, 2017). These micro-organisms decompose providing conducive environment for growth of vegetation (shrubs and mangroves). The fact that the study area is a delta; alludes that the process leading to this accretion is the gradual erosion of mto Tamamba bed. The accuracy of the results produced from the ground truthing exercise was 84% for Landsat and 88% for Sentinel-2 data. On the other hand, the validation results obtained via high resolution image (Sentinel-2) and resampled Landsat data gave an overall accuracy of 92%. Therefore, it can be concluded that validation via high spatial resolution data can aid in assessing impact of resolution on classification results. Field observation further confirms that areas with mangrove forest were less affected with erosion and accretion. This is because mangrove which are self-maintaining and naturally growing trees acts as line of defense against water tides and human activities.

5.13 Limitations

Prediction of future advancement of coastal geomorphological changes requires at least one historical data sets per year. The challenge of cloud cover on coastal areas like Kenya has made this unrealistic on Landsat data. Availability of consistence data provide reliable trends that aid in long-term analysis of patterns of coastal change. Aerial photos are better alternatives if taken below the clouds. However, challenge arises if photo of large area is to be taken at once. This study had a limitation of data gaps due to cloud cover. Landsat data having repeated coverage of 16 days could not provide a completely cloud free image forcing us to clip some areas susceptible to erosion and accretion for better analysis. Nevertheless, Sentinel-2 data fairly bridged the gap. High resolution data like SPOT could have offered the best alternative due to its early launch (22nd February,1986) and repeated coverage of 2-5 days; but they are costly. Despite these, this study was able to establish the shoreline alterations using satellite RS and GIS approaches.

Unavailability of information about coastal zone is another challenge. This has made it almost impossible to identifying vulnerable areas along the coastline. This poses challenge to the would be investors who need such information for right decision making. If such information is not availed a threat to economic development is eminent. This study can be a starting point for establishing a national coastline geodatabase on status of coastal ecosystem.

CHAPTER 6. CONCLUSION AND RECOMMENDATIONS.

6.1 Conclusion

This study acquired relevant satellite images (Landsat and Sentinel-2) from Earthexplorer despite the challenge of cloud cover. Using data retrieved from ROIs ('seeds') and spectral signature of predominant features in the image, endmember spectral library was developed. K-means clustering techniques aided in identification of these features during data training. The library consisted of five individual class files namely water, mangrove, shrubs, bare land and settlement. After which, image derived endmembers were used to classify the study area based on ML and SAM techniques.

ML algorithm proved superior than SAM producing an overall accuracy of 84% and 88% for Landsat and Sentinel-2 data respectively. The classification results were presented in thematic maps that revealed a prograding and receding land in this section of coastline. Change detection statistics of endmembers was generated and area coverage for each endmember tabulated for the period 1990-2021. The results revealed an increase in pixel coverage area of bare land and a decrease in area of water pixels. Temporal variation of endmembers was also presented in graphs and scatter plots. The correlation plots for endmember bare land and water gave $R^2 = 0.5138$ for Landsat data and $R^2 = 0.7857$ for Sentinel data.

This study went further and validated the resampled classified Landsat image with higher spatial resolution data (Sentinel-2) with an overall accuracy of 92%. The fact that a better validation results was obtained using high spatial resolution data suggests that resampling images to higher spatial resolution can aid in assessing impact of resolution on classified results.

From the aforementioned the objective of monitoring change in coastal morphology has been realized. This study has demonstrated that remote sensing and GIS can be used as a powerful tool in monitoring temporal and spatial change in coastal morphology.

6.2 Recommendations.

RS and GIS information have very great significance in terms of planning of coastal zones. Moreover, the application of these technologies would aid in the development of a robust mapping project and provide greater clarity on erosion risk areas for both public and private entities. Secondly information from such findings can be used by developers in making sound decision on where to erect coastal structures to prevent effects of land recession or plant more mangrove tree for defense. Thirdly, statistical findings can be used to create applied cartography of risk areas, such as maps of susceptible and vulnerable geo-hazards. Based on current findings it is recommended that Kenyan government should build structured walls along the coastline in land receding areas. Alternatively, more mangrove trees should be planted to minimize effect of tidal waves along the coastline. However, it should be noted that images of higher-resolution like IKONOS or SPOT may provide better alternative to this work by showing changes on the ground in greater details. Other supervised classification techniques like NDVI and minimum distance should be used to see which of the methods is more effective in detection of coastal morphology. Finally, future researchers should make full use of this technology and incorporate it into their studies of coastline change to address the challenge of cost and time wastage in field survey.

References

- Abuodha, P. a. W., Kairo, J.G., 2001. Human-induced stresses on mangrove swamps along the Kenyan coast. *Hydrobiologia* 458, 255–265. <https://doi.org/10.1023/A:1013130916811> (accessed on 6/6/2021)
- Ahmad, A., Quegan, S., 2012. Analysis of maximum likelihood classification on multispectral data. *Appl. Math. Sci.* 6, 6425–6436 <http://www.m-hikari.com/ams/ams-2012/ams-129-132-2012/ahmadAMS129-132-2012.pdf> (accessed on 1/6/2022).
- Alesheikh, A.A., Ghorbanali, A., Nouri, N., 2007. Coastline change detection using remote sensing. *Int. J. Environ. Sci. Technol.* 4, 61–66. <https://doi.org/10.1007/BF03325962> (accessed 2/23/2022)
- Berhane, T.M., Costa, H., Lane, C.R., Anenkhonov, O.A., Chepinoga, V.V., Autrey, B.C., 2019. The Influence of Region of Interest Heterogeneity on Classification Accuracy in Wetland Systems. *Remote Sens.* 11, 551. <https://doi.org/10.3390/rs11050551> (accessed 11/9/2021)
- Boak, E.H., Turner, I.L., 2005. Shoreline Definition and Detection: A Review. *J. Coast. Res.* 214, 688–703. <https://doi.org/10.2112/03-0071.1> (accessed 9/22/22)
- Burton, I., Lim, B., Spanger-Siegfried, E., Malone, E.L., Huq, S., 2005. Adaptation policy frameworks for climate change: developing strategies, policies, and measures. Cambridge University Press, Cambridge, UK ; New York.(Accessed 4/28/21)
- Camberlin, P., Planchon, O., 1997. Coastal Precipitation Regimes in Kenya. *Geogr. Ann. Ser. Phys. Geogr.* 79, 109–119.(accessed 11/9/2021)
- Carter, R.W.G., Woodroffe, C.D., 1997. Coastal Evolution: Late Quaternary Shoreline Morphodynamics. Cambridge University Press.(accessed 2/23/2022)
- Cenci, L., Santella, C., Laneve, G., Boccia, V., 2021. (PDF) Evaluating the Potentialities of Copernicus Very High Resolution (VHR) Optical Datasets for Assessing the Shoreline Erosion Hazard in Microtidal Environments [WWW Document]. URL https://www.researchgate.net/publication/354577120_Evaluating_the_Potentialities_of_Copernicus_Very_High_Resolution_VHR_Optical_Datasets_for_Assessing_the_Shoreline_Erosion_Hazard_in_Microtidal_Environments (accessed 7.31.22).
- Chaib, W., Guerfi, M., Hemdane, Y., 2020. Evaluation of coastal vulnerability and exposure to erosion and submersion risks in Bou Ismail Bay (Algeria) using the coastal risk index (CRI). *Arab. J. Geosci.* 13, 420. <https://doi.org/10.1007/s12517-020-05407-6>(accessed 2/6/2021)

Church, J.A., Clark, P.U., Cazenave, A., Gregory, J.M., Jevrejeva, S., Levermann, A., Merrifield, M.A., Milne, G.A., Nerem, R.S., Nunn, P.D., Payne, A.J., Pfeffer, W.T., Stammer, D., Unnikrishnan, A.S., 2013. Sea-Level Rise by 2100. *Science* 342, 1445–1445. <https://doi.org/10.1126/science.342.6165.1445-a>

Coppin, P.R., Bauer, M.E., 1996. Digital change detection in forest ecosystems with remote sensing imagery. *Remote Sens. Rev.* 13, 207–234. <https://doi.org/10.1080/02757259609532305>(accessed 12/1/2021)

Elsayed, M.A.K., Mahmoud, S.M., 2007. Groins System for Shoreline Stabilization on the East Side of the Rosetta Promontory, Nile Delta Coast. *J. Coast. Res.* 232, 380–387. <https://doi.org/10.2112/04-0319.1>(accessed 5/11/21)

Famiglietti, J.S., Devereaux, J.A., Laymon, C.A., Tsegaye, T., Houser, P.R., Jackson, T.J., Graham, S.T., Rodell, M., Oevelen, P.J. van, 1999. Ground-based investigation of soil moisture variability within remote sensing footprints During the Southern Great Plains 1997 (SGP97) Hydrology Experiment. *Water Resour. Res.* 35, 1839–1851. <https://doi.org/10.1029/1999WR900047>(accessed 2/23/2022)

Fan, D., Wu, Y., Zhang, Y., Burr, G., Huo, M., Li, J., 2017. South Flank of the Yangtze Delta: Past, present, and future. *Mar. Geol.* 392, 78–93. <https://doi.org/10.1016/j.margeo.2017.08.015>(accessed 9/12/2021)

Graham, D., Sault, M., Bailey, C.J., 2003. National Ocean Service Shoreline—Past, Present, and Future. *J. Coast. Res.* 14–32(accessed 11/9/2021).

Hoorweg, Muthiga, N., 2009. Advances in coastal ecology : people, processes and ecosystems in Kenya, African studies collection. African Studies Centre, Leiden. <https://www.ascleiden.nl/publications/advances-coastal-ecology-people-processes-and-ecosystems-kenya>.(4/28/2022)

Jensen, J.R., 1996. Introductory digital image processing: a remote sensing perspective. *Introd. Digit. Image Process. Remote Sens. Perspect.*<https://www.cabdirect.org/cabdirect/abstract/20001911540> (accessed 2/23/2022)

Johnson, U.K., 2013. River sediment supply, sedimentation and transport of the highly turbid sediment plume in Malindi Bay, Kenya. *J. Geogr. Sci.* 23, 465–489. <https://doi.org/10.1007/s11442-013-1022-x> (accessed 9/7/2021)

Kairo, J.G., 1995. Artificial regeneration and sustainable yield management of Mangrove forests at Gazi bay, Kenya (Thesis) <http://erepository.uonbi.ac.ke/handle/11295/25283>.(2/2/2023)

Kempka, D., Lackey, L., 1994. Using Remote Sensing to Detect and Monitor Land-Cover and Land-Use Change. [https://www.scrip.org/\(S\(351jmbntvnsjt1aadkposzje\)\)/reference/ReferencesPapers.aspx?ReferenceID=1757708](https://www.scrip.org/(S(351jmbntvnsjt1aadkposzje))/reference/ReferencesPapers.aspx?ReferenceID=1757708).(accessed 9/30/2022)

- Kevin White, H.M.E.A., 1999. Monitoring changing position of coastlines using Thematic Mapper imagery, an example from the Nile Delta. *Geomorphology* 93–105. [https://doi.org/10.1016/S0169-555X\(99\)00008-2](https://doi.org/10.1016/S0169-555X(99)00008-2)(accessed 10/2/2021)
- Kimani, E., Okemwa, G., Okello, J., Kairo, J., Nina, W., Ochiwo, J., Mirera, D., Mwaura, J., Kamau, J., Kosore, C., Ong'anda, H., Magori, C., Kimeli, A., Okuku, E., 2017. State of Coast Report for Kenya (Second Edition) Enhancing Integrated Management of Coastal and Marine Resources in Kenya. (2/9/2022)
- Kitheka, J.U., Obiero, M., Nthenge, P., 2005. River discharge, sediment transport and exchange in the Tana Estuary, Kenya. *Estuar. Coast. Shelf Sci., Science for management in the western Indian Ocean* Science for management in the western Indian Ocean 63, 455–468. <https://doi.org/10.1016/j.ecss.2004.11.011>(accessed 12/09/2021)
- Klemas, V., 2010. Remote Sensing Techniques for Studying Coastal Ecosystems: An Overview. *J. Coast. Res.* 27, 2–17. <https://doi.org/10.2112/JCOASTRES-D-10-00103.1>(accessed 1/6/2022)
- Kong, D., Miao, C., Borthwick, A.G.L., Duan, Q., Liu, H., Sun, Q., Ye, A., Di, Z., Gong, W., 2015. Evolution of the Yellow River Delta and its relationship with runoff and sediment load from 1983 to 2011. *J. Hydrol.* 520, 157–167. <https://doi.org/10.1016/j.jhydrol.2014.09.038> (accessed 23/7/2021)
- Kostiuk, M., Geography, M., 2002. Using Remote Sensing Data to Detect Sea Level Change. *Conf. Proc.* 9 <https://www.isprs.org/proceedings/xxxiv/part1/paper/00106.pdf>.(accessed 8/3/2021)
- Kuleli, T., Guneroglu, A., Karsli, F., Dihkan, M., 2011. Automatic detection of shoreline change on coastal Ramsar wetlands of Turkey. *Ocean Eng.* 38, 1141–1149. <https://doi.org/10.1016/j.oceaneng.2011.05.006>
- Latawiec, A., Agol, D., 2015. Sustainability Indicators in Practice. *De Gruyter Open Poland.* <https://doi.org/10.1515/9783110450507>
- Latella, M., Luijendijk, A., Moreno-Rodenas, A.M., Camporeale, C., 2021. Satellite Image Processing for the Coarse-Scale Investigation of Sandy Coastal Areas. *Remote Sens.* 13, 4613. <https://doi.org/10.3390/rs13224613>
- Leatherman, S.P., Zhang, K., Douglas, B.C., 2000. Sea level rise shown to drive coastal erosion. *Eos Trans. Am. Geophys. Union* 81, 55. <https://doi.org/10.1029/00EO00034>
- Leone, F., Lavigne, F., Paris, R., Denain, J.-C., Vinet, F., 2011. A spatial analysis of the December 26th, 2004 tsunami-induced damages: Lessons learned for a better risk assessment integrating buildings vulnerability. *Appl. Geogr.* 31, 363–375. <https://doi.org/10.1016/j.apgeog.2010.07.009>
- Li, X., Damen, M.C.J., 2010. Coastline change detection with satellite remote sensing for environmental management of the Pearl River Estuary, China. *J. Mar. Syst., Pearl River Estuary related sediments as*

response to Holocene climate change and anthropogenic impact (PECAI) 82, S54–S61.
<https://doi.org/10.1016/j.jmarsys.2010.02.005>

Lillesand, T., Kiefer, R.W., Chipman, J., 2015. Remote Sensing and Image Interpretation. John Wiley & Sons <https://www.wiley.com/en-ie/Remote+Sensing+and+Image+Interpretation,+7th+Edition-p-9781118343289>.

Liu, H., 2009. Shoreline Mapping and Coastal Change Studies Using RemoteSensing Imagery and LIDAR Data, in: Yang, X. (Ed.), Remote Sensing and Geospatial Technologies for Coastal Ecosystem Assessment and Management, Lecture Notes in Geoinformation and Cartography. Springer, Berlin, Heidelberg, pp. 297–322. https://doi.org/10.1007/978-3-540-88183-4_13

Lobell, D.B., 2010. Remote Sensing of Soil Degradation: Introduction. J. Environ. Qual. 39, 1. <https://doi.org/10.2134/jeq2009.0326>

Lobell, D.B., Lesch, S.M., Corwin, D.L., Ulmer, M.G., Anderson, K.A., Potts, D.J., Doolittle, J.A., Matos, M.R., Baltes, M.J., 2010. Regional-scale Assessment of Soil Salinity in the Red River Valley Using Multi-year MODIS EVI and NDVI. J. Environ. Qual. 39, 35–41. <https://doi.org/10.2134/jeq2009.0140>

Lu, D., Mausel, P., Brondízio, E., Moran, E., 2004. Change detection techniques. Int. J. Remote Sens. 25, 2365–2401. <https://doi.org/10.1080/0143116031000139863>

MacDonald, J., 2017. When the Sea Recedes [WWW Document]. JSTOR Dly. URL <https://daily.jstor.org/when-the-sea-recedes/> (accessed 8/3/22).

Macleod, R.D., Congalton, R.G., 1998. A Quantitative Comparison of Change-Detection Algorithms for Monitoring Eelgrass from Remotely Sensed Data 10 <https://www.semanticscholar.org/paper/A-Quantitative-Comparison-of-Change-Detection-for-Macleod-Congalton/151abe1f26941f0566e0ce4ee3155833c31afe79>.(accessed 9/22/2022)

Maiti, S., Bhattacharya, A.K., 2009. Shoreline change analysis and its application to prediction: A remote sensing and statistics based approach. Mar. Geol. 257, 11–23. <https://doi.org/10.1016/j.margeo.2008.10.006>(accssed 6/12/2021)

Mani Murali, R., Ankita, M., Amrita, S., Vethamony, P., 2013. Coastal vulnerability assessment of Puducherry coast, India, using the analytical hierarchical process. Nat. Hazards Earth Syst. Sci. 13, 3291–3311. <https://doi.org/10.5194/nhess-13-3291-2013>(accessed 10/2/2021)

Morton, R., Gibeaut, J., Paine, J., 1995. Meso-scale transfer of sand during and after storms: implications for prediction of shoreline movement. Mar. Geol. 126. [https://doi.org/10.1016/0025-3227\(95\)00071-6](https://doi.org/10.1016/0025-3227(95)00071-6)(accessed 3/4/2021)

Morton, R.A., Speed, F.M., 1998. Evaluation of Shorelines and Legal Boundaries Controlled by Water Levels on Sandy Beaches. J. Coast. Res. 14, 1373–1384 (accessed 2/23/2022).

- Mukhopadhyay, A., Mukherjee, Sandip, Mukherjee, Samadrita, Ghosh, S., Hazra, S., Mitra, D., 2012. Automatic shoreline detection and future prediction: A case study on Puri Coast, Bay of Bengal, India. *Eur. J. Remote Sens.* 45, 201–213. <https://doi.org/10.5721/EuJRS20124519>(accessed 10/2/2021)
- Munyao, T.M., 1993. Environmental effects of Coastal Sedimentation: A Case study fo Shirazi-Funzi Lagoon (Report) <https://aquadocs.org/handle/1834/334?show=full> (2/23/2022).
- Odada, 1993. The problem of coastal erosion and flooding in Eastern Africa <http://erepository.uonbi.ac.ke/handle/11295/49149> [WWW Document].(accessed 11/9/2021)
- Odada, E., 2010. Integration of coastal and marine areas into sustainable development strategies: A case study of Africa https://www.researchgate.net/publication/229029215_Integration_of_coastal_and_marine_areas_into_sustainable_development_strategies_A_case_study_of_Africa.(accessed 8/5/2021)
- Odada, E., 2001. Contribution of Africa’s Coastal and Marine Sectors to Sustainable Development <http://erepository.uonbi.ac.ke/handle/11295/73327>.(accessed 2/23/2022)
- Omuombo, C.A., Olago, Daniel O., Odada, E.O., 2013. Chapter 22 - Coastal Erosion, in: Paron, P., Olago, Daniel Ochieng, Omuto, C.T. (Eds.), *Developments in Earth Surface Processes, Kenya: A Natural Outlook*. Elsevier, pp. 331–339. <https://doi.org/10.1016/B978-0-444-59559-1.00022-0>(accessed 2/23/2022)
- Ondieki, J.O., Mito, C.O., Kaniu, M.I., 2022. Feasibility of mapping radioactive minerals in high background radiation areas using remote sensing techniques. *Int. J. Appl. Earth Obs. Geoinformation* 107, 102700. <https://doi.org/10.1016/j.jag.2022.102700>(accessed 5/03/2023)
- Richards, J.A., 2013. Supervised Classification Techniques, in: *Remote Sensing Digital Image Analysis*. Springer Berlin Heidelberg, Berlin, Heidelberg, pp. 247–318. https://doi.org/10.1007/978-3-642-30062-2_8 (accessed 10/2/2021)
- Saravanan, S., Chandrasekar, N., Rajamanickam, M., Hentry, C., Jovivek, V., 2014. Management of Coastal Erosion Using Remote Sensing and GIS Techniques (SE India). *Int. J. Ocean Clim. Syst.* 5, 211–221. <https://doi.org/10.1260/1759-3131.5.4.211> (accessed 10/2/2021)
- Şener, Ş., Şener, E., Nas, B., Karagüzel, R., 2010. Combining AHP with GIS for landfill site selection: A case study in the Lake Beyşehir catchment area (Konya, Turkey). *Waste Manag.* 30, 2037–2046. <https://doi.org/10.1016/j.wasman.2010.05.024> (accessed 8/03/2022)
- SINGH, A., 1989. Review Article Digital change detection techniques using remotely-sensed data. *Int. J. Remote Sens.* 10, 989–1003. <https://doi.org/10.1080/01431168908903939> (accessed 2/23/2022)
- Sivakumar, M., Roy, p, Harmsen, K., 2003. *Satellite Remote Sensing and GIS Application in Agriculture Meterolgy*.

https://www.researchgate.net/publication/276283296_Satellite_Remote_Sensing_and_GIS_Applications_in_Agriculture_Meteorology (accessed 8/3/2021)

Sridhar, R.S., Elangovan, K., Suresh, P.K., 2009. Long Term Shoreline Oscillation and Changes of Cauvery Delta Coastline Inferred from Satellite Imageries. *J. Sustain. Dev.* 2, p132. <https://doi.org/10.5539/jsd.v2n1p132>(accessed 10/2/2021)

Wang, X.-Z., Zhang, H.-G., Fu, B., Shi, A., 2013. Analysis on the coastline change and erosion-accretion evolution of the Pearl River Estuary, China, based on remote-sensing images and nautical charts. *J. Appl. Remote Sens.* 7, 073519. <https://doi.org/10.1117/1.JRS.7.073519>(accessed 8/4/2021)

White, K., El Asmar, H.M., 1999. Monitoring changing position of coastlines using Thematic Mapper imagery, an example from the Nile Delta. *Geomorphology* 29, 93–105. [https://doi.org/10.1016/S0169-555X\(99\)00008-2](https://doi.org/10.1016/S0169-555X(99)00008-2)(accessed 10/2/2021)

Wilson, E.O., 2010. *The Diversity of Life: With a New Preface*, 2nd edition. ed. Belknap Press: An Imprint of Harvard University Press, Cambridge, Mass. (2/24/2023)